Marine Geology 420 (2020) 106089

Contents lists available at ScienceDirect

Marine Geology

journal homepage: www.elsevier.com/locate/margo

Spatial and seasonal variability in grain size, magnetic susceptibility, and organic elemental geochemistry of channel-bed sediments from the Mekong Delta, Vietnam: Implications for hydro-sedimentary dynamic processes

Yamei Jiang[a,b], Yoshiki Saito[c,d], Thi Kim Oanh Ta[e], Zhanghua Wang[a,b,f,*], Marcello Gugliotta[c], Van Lap Nguyen[e]

[a] State Key Laboratory of Estuarine and Coastal Research, East China Normal University, Shanghai 200062, China
[b] Institute of Urban Development, East China Normal University, Shanghai 200062, China
[c] Estuary Research Center, Shimane University, 1060 Nishikawatsu-cho, Matsue 690-8504, Japan
[d] Geological Survey of Japan, AIST, Central 7, Higashi 1-1-1, Tsukuba 305-8567, Japan
[e] HCMC Institute of Resources Geography, VAST, Ho Chi Minh City, Viet Nam
[f] Southern Laboratory of Ocean Science and Engineering (Guangdong, Zhuhai), Zhuhai 519000, China

ARTICLE INFO

Editor: Edward Anthony

Keywords:
Sediment source
Sediment trapping
River-mouth sediment dynamics
Salinity intrusion
Fluvial–marine transition zone

ABSTRACT

Understanding the relationship between depositional processes and their products in the fluvial–marine transition zone in tide-dominated depositional systems is fundamental to improving environmental and stratigraphic interpretations of long-term sedimentary records. The distributary channels of the Mekong Delta represent a typical example of a complex sedimentary environment characterized by strong fluvial and tidal interactions, and seasonal variability in hydro-sedimentary dynamic processes, particularly the migration of a salt wedge front linked to seasonal fluctuations in freshwater discharge. For this study, we analyzed grain size, magnetic susceptibility, and organic elemental geochemistry of channel-bed surficial sediments collected in 2015 from all distributary channels during the dry season and from the Mekong–Co Chien River during the flood season. This paper reports spatial and seasonal differences in the characteristics of channel-bed surficial sediments, which are closely linked to sediment sources and depositional processes during the dry and flood seasons.

Distributary channels are characterized by coarse-grained sediments in the upper reaches and fine-grained sediments in the lower reaches, in both dry and flood seasons, reflecting the difference between the upstream fluvial-dominated environment and the downstream tide-dominated environment. Flood season samples from the Co Chien River show higher magnetic mineral contents and a terrestrial source of organic carbon compared with dry season samples, indicating sourcing from the drainage basin and trapping of suspended materials in the distributary channel due to the barrier effect of the saltwater wedge at the river mouth. Compared with the flood season, during the dry season the mud content was lower in the downstream reach close to the river mouth and higher in the upstream reach of the Co Chien River, and the content of magnetic minerals was lower in both reaches, indicating dissolution of magnetic minerals during early diagenesis. Furthermore, the lower C/N ratios (< 10) and slightly enriched $\delta^{13}C$ values of the dry season samples from the Co Chien River imply an additional contribution of organic carbon from a marine source. These various features imply a landward import of mud into the Co Chien River induced by stronger salinity intrusion during the dry season. Along the downstream tract of the Bassac River, two mud-dominated reaches were identified during the dry season. The magnetic mineral contents, C/N ratios and $\delta^{13}C$ values indicate that the mud-dominated reach near the Bassac River mouth is also supplied from resuspended sediments by estuarine circulation and tidal pumping, whereas the mud in the reach that is transitional from fluvial to tide dominance has a riverine supply. The results suggest that the Mekong distributary channels are important sinks for suspended sediments during both the flood and dry seasons, controlled by a sediment trapping mechanism provided by either estuarine processes or the morphological configuration of the channels, both of which are controlled by fluvial–tidal dynamics. These depositional processes may be compensating for the incision of channels induced by sand mining in recent decades.

* Corresponding author at: State Key Laboratory of Estuarine and Coastal Research, East China Normal University, Shanghai 200062, China.
E-mail address: zhwang@geo.ecnu.edu.cn (Z. Wang).

https://doi.org/10.1016/j.margeo.2019.106089
Received 31 January 2019; Received in revised form 19 November 2019; Accepted 21 November 2019
Available online 28 November 2019
0025-3227/

1. Introduction

The fluvial-to-marine transition zone (i.e., the zone of interaction between riverine and marine processes in coastal rivers) is characterized by high sedimentation rates, with deposits in this zone constituting important archives for reconstructing geological histories at various scales from local to continental (Nittrouer et al., 2007). However, difficulties in interpreting such archives have hindered a comprehensive understanding of environmental change based on such records. In particular, tide-dominated river mouths are especially complex, making recognition of stratigraphic architecture extremely difficult (Dalrymple and Choi, 2007). Studies of the relationship between depositional processes and their products in present-day transition zones should help to explain high-frequency dynamics such as tidal asymmetry and estuarine circulation induced by salinity intrusion that are contained in sedimentary records. Such information would allow the bridging of time-scale-based investigations (such as long-term stratigraphic and morphological studies) with numerical models (e.g., Nittrouer et al., 2007; Gao and Collins, 2014).

The salt wedge movement in both tidal and seasonal cycles and associated estuarine circulation is among the most important hydro-sedimentary dynamic processes in the tide-dominated estuaries (Geyer, 1988), because the estuarine circulation, together with the tidal propagation play critical roles in the formation of estuarine turbidity maxima and the trapping of suspended particulates in the fluvial-to-marine transition zone (Burchard et al., 2018). In recent years, much work has focused on the tidal asymmetry and estuarine circulation and their link to suspended sediment dispersal and entrapment in tide-dominated river mouths (e.g., Ashworth et al., 2015; Freitas et al., 2017; Nittrouer et al., 2017a; Ogston et al., 2017a; Asp et al., 2018; Burchard et al., 2018; Sandbach et al., 2018; Gugliotta and Saito, 2019). These studies have revealed that seasonal displacement of the estuarine turbidity maximum can occur as a result of changes in freshwater discharge in a monsoonal setting (Nowacki et al., 2015; Asp et al., 2018). In addition, the locations of estuarine turbidity maxima and mud deposition may lie upstream, far from the coastline, because of a strong tidal influence (Freitas et al., 2017). By contrast, only a few systematic examinations have been made of the spatial and seasonal variability in the channel-bed surficial sediments controlled by these hydro-sedimentary dynamic processes in fluvial–tidal transition zones.

The Mekong Delta (Fig. 1) is characterized by one of the highest river discharges in the world, which changes seasonally on account of the monsoonal regime and a strong tidal function, making it an ideal system in which to investigate interactions between riverine and marine processes and their effects on sedimentation. Previous studies have revealed marked seasonal differences in hydro-sedimentary dynamic processes and associated delivery or trapping of suspended sediments in the Bassac River (Fig. 1B), which is the major distributary channel of the Mekong Delta and discharges the largest individual volume of freshwater from the Mekong River into the sea (Wolanski et al., 1996; Wolanski et al., 1998; Nowacki et al., 2015; McLachlan et al., 2017; Nittrouer et al., 2017b; Thanh et al., 2017). In contrast, knowledge about hydro-sedimentary dynamic processes in other distributary channels of the Mekong Delta is still limited, and these processes could differ from those of the Bassac River because of the lower freshwater discharges occurring as a result of the higher number of channel bifurcations (Fig. 1B; Nguyen et al., 2008).

Several recent studies have investigated channel-bed sediments with respect to the morphological configuration of distributary channels across the Mekong Delta (Gugliotta et al., 2017, 2018, 2019; Gugliotta and Saito, 2019). Those studies emphasized the tidal influence on both channel morphology and the distribution of channel-bed sediments, and divided the distributary channels into fluvial-dominated upstream and tide-dominated downstream tracts. In addition, a novel attempt was made to link sediment type to hydro-sedimentary dynamic processes at a seasonal scale (Gugliotta et al., 2019). In the present study, we further analyze the characteristics of these channel-bed surficial sediments collected during the dry and flood seasons of 2015 (Gugliotta et al., 2017). By analyzing sediment grain size, magnetic susceptibility, and organic elemental and isotopic composition, we investigate the spatial and seasonal variations in sediment properties to identify the different sediment sources and draw implications for hydro-sedimentary dynamic processes. In particular, on the basis of the channel-bed sediment properties, we aim to identify and explain seasonal differences in hydro-sedimentary dynamic processes in those distributary channels that are supplied by lesser freshwater discharge, so that to compare with those of the Bassac River reported by previous studies. The results should provide an analog for predicting the future evolution of tide-dominated distributary channels experiencing relative sea-level rise. Our study also provides insights into the process–product relationship at a seasonal scale in a tidal river environment in a monsoonal setting.

2. Study area

2.1. Regional setting

The Mekong River originates from the Tibetan Plateau, flows southward through six countries (China, Myanmar, Laos, Thailand, Cambodia, and Vietnam), and enters the South China Sea (also known as the East Sea in Vietnam; Fig. 1a, b). At ~4800 km long, the river is the 12th longest in the world (Wang et al., 2011b). The major part of the Mekong drainage basin is located in the Asian tropical monsoon region, with the northeast monsoon prevailing from November to March, and the southwest monsoon from May to late September or early October. In the basin, the rainy season lasts from May to October and the dry season from November to April. However, regulation by Tonle Sap Lake (Fig. 1A) means that the high flow in the delta region occurs from September to November (Mekong River Commission, 2005). The freshwater discharge attains its highest level in October (e.g., 36,700 m^3/s at Phnom Penh in Cambodia; Gugliotta et al., 2019) and generally drops to its lowest level in April (e.g., ~2000 m^3/s at Tan Chau and Chau Doc in Vietnam; Fig. 1B; Tri, 2012).

The Mekong Delta lies between Phnom Penh and the southern coast of Vietnam (Fig. 1A). Its delta plain covers ~62,500 km^2 (Nguyen et al., 2000), making it the third largest in the world. The Mekong River bifurcates into two main distributary channels at Phnom Penh, namely, the Mekong and Bassac rivers as the eastern and western branches, respectively (Fig. 1B). The freshwater discharge recorded by the hydrologic station at Tan Chau in the Mekong River is much higher than that at Chau Doc in the Bassac River (Fig. 1B; Mekong River Commission, 2005). However, a considerable portion of the freshwater discharge of the Mekong River passes through the Vam Nao River into the Bassac River. Thus, the freshwater discharge of the two branches is similar, as recorded by the hydrologic stations at My Thuan and Can Tho (Fig. 1B; Tri, 2012). The Mekong River bifurcates into the Co Chien and My Tho distributaries about 100 km upstream of the river mouth (b3 in Fig. 1B), with the My Tho further subdividing into multiple distributary channels (Ham Luong, Cua Tieu, Cua Dai, and Ba Lai), of which the Ba Lai River is abandoned (Tamura et al., 2012a, 2012b). The Bassac River bifurcates into a pair of distributary channels with two river mouths at Dinh An and Tran De, respectively, at a distance of about 40 km from the river mouth (b5 in Fig. 1B). The channel at Dinh An has the highest individual discharge of freshwater from the Mekong drainage basin, constituting about 41.8% during the dry season (Nguyen et al., 2008). In contrast, the Co Chien River discharges only about 18.3% of the freshwater during the dry season (Nguyen et al., 2008). Salt intrusion occurs in all distributary channels up to 50–65 km upstream of the river mouth during the dry season (Fig. 1C). During the flood season, there is only an intermittent presence of a saltwater wedge at the river mouth of the Bassac River (Ogston et al., 2017a, 2017b), whereas the intrusion distance is about 15–30 km in other distributary channels (Gagliano and McIntire, 1968; Nguyen et al., 2008; Gugliotta

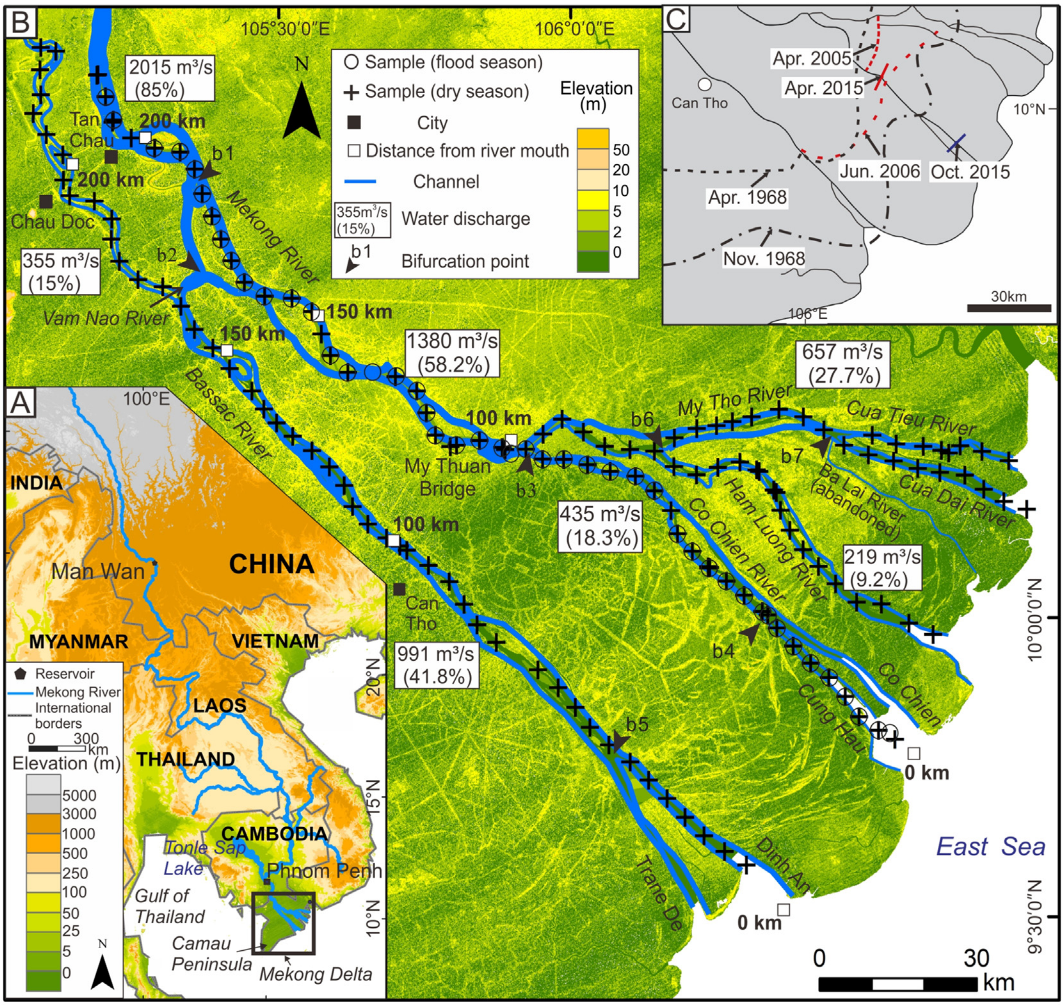

Fig. 1. (A) Digital elevation model and location of the Mekong Delta. (B) Sampling locations during the dry and flood seasons in 2015. Also indicated are the distance to the river mouth along the Mekong–Co Chien and Bassac rivers and the freshwater discharge and associated percentages of the total freshwater discharge through each distributary channel during the dry season (Nguyen et al., 2008). Tran De, Dinh An, Cung Hau, and Co Chien are the four river mouths of the Bassac and Co Chien rivers. The base maps in (A) and (B) were generated with ArcGis 10.1 software using the topographic dataset provided by the Geospatial Data Cloud site, Computer Network Information Center, Chinese Academy of Sciences (http://www.gscloud.cn). (C) Saltwater intrusion in the Mekong Delta in different years. Data source: Apr. and Nov. 1968, Gagliano and McIntire (1968); Apr. 2005 and Jun. 2006, Nguyen et al. (2008); Apr. and Oct. 2015, Gugliotta et al. (2017). (For interpretation of the references to colour in this figure legend, the reader is referred to the web version of this article.)

et al., 2017). Although the number of artificial reservoirs in the drainage basin has increased significantly since the 1990s (Kummu and Varis, 2007), the distance of salt intrusion into the delta plain appears to have undergone only limited change (Fig. 1c; Gagliano and McIntire, 1968; Nguyen et al., 2008; Gugliotta et al., 2017).

The Mekong Delta was tide-dominated during the middle Holocene but evolved into a combined wave- and tide-dominated system about 3000 years ago, which persists today (Ta et al., 2002, 2005; Tamura et al., 2010). At present, the Mekong Delta is affected by mixed diurnal and semi-diurnal tides. The amplitudes of the semi-diurnal M2 and fortnightly S2 tides are 0.9 m and 0.5 m, respectively, whereas the amplitudes of the K1 and O1 tides are 0.7 m and 0.5 m, respectively (Nguyen, 2013). Irregular semi-diurnal tides prevail at the river mouth with a mean tidal range of 2.5 ± 0.1 m and a maximum tidal range of ~3.3–3.7 m (Nguyen, 2013). Tide-generated water-level fluctuations are observed at least up to Phnom Penh (Cambodia), > 300 km upstream of the respective river mouths (Gugliotta et al., 2017). The influence of waves is confined to the coastline and offshore area, and is closely related to the monsoon (Tamura et al., 2010). In addition, wave directions are consistent with the wind, approaching mainly from the east-northeast during November–March and from the west-southwest between June and September. The monthly mean effective wave height is 0.8–1.2 m in winter and 0.5–0.6 m in summer (Dee et al., 2011; Gugliotta et al., 2017). The stronger waves of the winter monsoon resuspend the mud deposited during the flood season in coastline and the subaqueous delta and generate a longshore current with a southwestward net sediment transport to the Camau Peninsula (e.g., Nguyen et al., 2000; Kanai et al., 2013a, 2013b; Nittrouer et al., 2017b).

Prior to the 1990s, the Mekong River transported 145–160 Mt/yr of suspended sediments to the river mouth (Milliman and Meade, 1983). However, it was estimated that the total suspended sediment load would reduce by 51% owing to the sediment trapping in the 38 reservoirs that have been built or are under construction in the drainage basin (Kondolf et al., 2014). River-bed mining has been intensified in the main channels of both the drainage basin and delta region in recent decades. The river-bed mining occurred mainly in the low-flow season, with an estimated total amount of 55.2 Mt. (34.5 million m^3) of sediments being extracted from the Mekong main channel in the middle and lower drainage basin in 2011 (Bravard et al., 2013). In the delta plain, Brunier et al. (2014) reported that 90 and 110 million m^3 of channel-bed aggregates were removed from the Mekong and Bassac rivers from 1998 to 2008, respectively, and that the mining induced marked morphological changes that were not in equilibrium with natural hydro-sedimentary dynamics.

C_3 plants including broadleaf deciduous forest and rice dominate in the middle and lower Mekong drainage basin and delta region (Mekong River Commission, 2010), whereas rangeland prevails in the upper basin (Allison et al., 2017a). Broadleaved deciduous forest accounts for 30% and paddy rice for 22% of the basin's land cover (Mekong River Commission, 2010). Mangroves including *Sonneratia*, *Nypa*, and *Avicennia* grow along the river banks of the lower reaches of the distributary channels in the delta region (Gugliotta et al., 2017). In addition, some C_4 plants, including the sugar cane and corn, are planted in the lowland and levee of the delta region, respectively.

2.2. Hydro-sedimentary dynamics in the Bassac River

The Bassac River can be divided into two major regimes, namely, tidal river (the freshwater reach) and estuary (the brackish water reach), according to the distribution of salinity (McLachlan et al., 2017; Nittrouer et al., 2017a; Ogston et al., 2017b). As a result of the monsoonal climate and associated variations in the volume of freshwater discharge, the boundaries of these two regimes have marked seasonal displacements. Previous studies have developed a conceptual model of the hydro-sedimentary dynamic processes in the Bassac River at a seasonal scale (Wolanski et al., 1996; Nowacki et al., 2015; McLachlan et al., 2017; Ogston et al., 2017b), summarized as follows. During the flood season, salt intrusion into the downstream tract of the Bassac River occurs only intermittently and forms a pronounced stratification of the water column near the mouth because of the large volume of runoff. Therefore, fine-grained suspended sediment is transported mainly to the delta front, with only the sandy component being deposited in the Bassac River. Estuarine circulation occurs together with the intermittent appearance of the saltwater wedge, and a zone of maximum turbidity is only formed at the toe of the saltwater wedge at flood tide (Wolanski et al., 1996). During the dry season, owing to the weakening of freshwater discharge, salt intrusion exceeds 40 km inland (Fig. 1C; McLachlan et al., 2017), and the lower reach of the Bassac River becomes a partially mixed estuary. Under the combined functions of tidal asymmetry and estuarine circulation, fine-grained particulates resuspended from coastal zones of the delta are imported into the Bassac River and deposited in the channel with a thickness of 0.25–1.00 m (Wolanski et al., 1998; Allison et al., 2017b; McLachlan et al., 2017). McLachlan et al. (2017) further suggested that there is an interface zone between the tidal river and the estuary, where the suspended particulates carried by the runoff and imported by the tidal current and estuarine circulation converge. In addition, fine-grained particulates are easily settled and deposited in the channel on account of the weakening of near-bed shear stress in the interface zone. The mud deposits can therefore reach many kilometers upstream of the estuarine regime during the dry season (McLachlan et al., 2017).

3. Materials and methods

A total of 199 surficial sediment samples were collected from the beds of distributary channels of the Mekong Delta during the dry (January–May) and flood (October) seasons in 2015 (Table 1; Gugliotta et al., 2017). Dry-season samples (152) were collected across five distributary channels, whereas flood-season samples (47) were collected along the Mekong and Co Chien rivers to the mouth of the Cung Hau (Fig. 1B). No samples were collected from the Bassac River during the flood season because little sedimentation occurs there during this season (Wolanski et al., 1996; Nowacki et al., 2015; McLachlan et al., 2017; Ogston et al., 2017b). All samples were taken from the mid-point of the river width with a KS grab sampler (15 cm × 15 cm, 2.7 l, Rigo; Gugliotta et al., 2017). The location of each sample was recorded with a Garmin GPSMAP 64 s, and water depth was measured synchronously using a portable hand-held depth sounder (PS-7, Honda Electronics) (Gugliotta et al., 2017).

Sediment grain-size analysis was performed on 196 samples; the remaining three did not have sufficient quantities of sediment. Of the 196 samples, 11 from the Mekong and Bassac rivers contained gravel components, which were excluded during sample pretreatment. All 199 samples were tested for magnetic susceptibility, including mass susceptibility (χ_{lf}, 10^{-8} m^3 kg^{-1}) and frequency-dependent susceptibility (χ_{fd}, %). Organic elemental geochemical compositions were analyzed for 146 samples consisting mainly of fine-grained particles as determined visually.

The samples for grain size analysis were firstly thoroughly mixed and dried at 40 °C, and then a subsample of about 0.2 g was taken from each sample. To remove organic matter and carbonate, 5 ml H_2O_2 (10%) and 5 ml HCl (10%) were added sequentially to each sample. After thorough reaction achieved by heating on an electric hot plate, each sample was washed with distilled water, followed by adding 5 ml 5% $Na(PO_3)_6$ to prevent flocculation. After shaking in an ultrasonic bath for 15 min, the grain size distribution of each sample was measured using a Beckman laser particle size analyzer (LS13320, Coulter, USA) at the State Key Laboratory of Estuarine and Coastal Research, East China Normal University, Shanghai, China.

About 10 g of sediment from each sample was taken for magnetic susceptibility measurements. These subsamples were weighed and wrapped with film after drying at 38 °C. The low-frequency (465 Hz, LF) and high-frequency (4650 Hz, HF) susceptibilities were measured for each subsample using a Bartington MS2B sensor (errors of 0.49% and 0.57% of the measured values for LF and HF, respectively, based on replicated measurements, $n = 7$). The mass magnetic susceptibility (χ_{lf}, 10^{-8} m^3 kg^{-1}) and the frequency-dependent susceptibility (χ_{fd}, %) were calculated as follows:

$$\chi_{lf} = \mathrm{LF/Mass} \tag{1}$$

$$\chi_{fd} = ((\chi_{lf} - \chi_{hf})/\chi_{lf}) \times 100 \tag{2}$$

Sample preparation for organic geochemical analysis was as follows. Samples were first freeze-dried for 72 h, then 6 g of sediment was taken from each sample and ground with an agate mortar to pass through a 200-mesh sieve. The sieved sample was divided into two groups, A and B, at a mass ratio of about 2:1. Group B material was wrapped for measurement of total carbon (TC) and total nitrogen (TN). Group A material was placed in a centrifuge tube, immersed in 20 ml 1 mol/l HCl overnight, and the centrifuge tube containing the sample was then placed in a water bath (60 °C) for 30 min to remove carbonate. The sample was further washed with ultrapure water until the pH of the

Table 1
Sampling information including the sampling times and number of samples for each distributary channel of the Mekong Delta.

Sampling time		Bassac River	Mekong River	Co Chien River	My Tho River	Ham Luong River	Cua Dai River	Cua Tieu River
Dry season	2015.01.18–2015.01.19				2			8
	2015.02.05–2015.02.07				4	18		
	2015.03.14–2015.03.24	29	29	24	3			
	2015.05.07–2015.05.13	19	2		6		8	
	Total in dry season	48	31	24	15	18	8	8
Flood season	2015.10.21–2015.10.27		25	22				

supernatant reached neutral. After centrifugation, the sample was dried, ground, and divided into two parts for measuring total organic carbon (TOC) and stable isotope $\delta^{13}C$, respectively. Measurements of TC, TOC, and TN were completed at the State Key Laboratory of Estuarine and Coastal Research, East China Normal University, using a Vario Cube elemental analyzer (Elementar, Germany) and calibrated with national geochemical reference standard GSD-9 (error < 0.5% of the measured value). $\delta^{13}C$ values were measured using a Delta V Advantage mass spectrometer (reference materials: Urea#2 and Acetanilide#1; error < 0.2‰ based on replicated measurements, $n = 5$) at the Third Institute of Oceanography of the State Oceanic Administration, Xiameng, China. C/N was calculated using the weight ratio between TOC and TN.

4. Spatial and seasonal variations in channel-bed surficial sediments

4.1. Grain size

Overall fining and muddying trends were observed from upstream reaches to downstream reaches for both flood and dry seasons (Figs. 2, 3a, 4a–d). For example, mud content was mostly < 30% and the median grain size ranged mostly from 200 to 300 μm in the upper reach of the Bassac River during the dry season (Fig. 2a, b). Mud content increased in the downstream direction in the lower reach at a distance of about 120 km from the river mouth, accounting for 20%–90% of the total sediment in the river section located 110–80 km from the river mouth (Tr reach between the upstream and downstream tracts of the Bassac River in Fig. 2a; Gugliotta et al., 2017). In the reach close to the river mouth of Dinh An (downstream of b5; Fig. 1B; D-A reach in Fig. 2a), the mud content further increased to values > 60% and the highest reached 95.5% in some locations. Median grain sizes were mostly < 50 μm in the two mud-dominated reaches. Furthermore, the average median grain size in the D-A reach was 76 μm, much finer than that of 190 μm in the Bassac River (Table 2; Fig. 4d).

In the Mekong River (upstream of b3; Fig. 2c), the mud content was ≤30% (mean of 24%) and the median grain size was 128–381 μm (mean of 225 μm) during the dry season (Table 2). Downstream of b3, in the Co Chien, Co Chien–Cung Hau, Ham Luong, My Tho, Cua Dai, and Cua Tieu reaches, the channel-bed surficial sediments were mud dominated, with mean mud contents of > 50% during the dry season (Fig. 2c–h). The average median grain size was 51–75 μm in the Co Chien–Cung Hau, My Tho, Cua Dai, and Cua Tieu reaches, and was 90 μm and 88 μm in the Co Chien and Ham Luong reaches, respectively (Table 2). During the flood season, the channel-bed surficial sediments in the Mekong River were composed mainly of sand, whereas the mud content was < 20%, except for a few samples that consisted of 30%–50% mud about 150–100 km from the river mouth (Fig. 2c). The median grain size ranged from 250 to 400 μm in the river reach upstream of b1 and decreased to 100–300 μm in the reach between b1 and b3 (Fig. 2d). The mean sand content was 58.2% in the Co Chien reach (between b3 and b4) in the flood season, clearly lower than the 83.2% recorded in the Mekong River. The average median grain size was 122 μm in the Co Chien reach. In the Co Chien–Cung Hau reach (downstream of b4), the mean sand content was 27.2% and the median grain size was only 53 μm on average (Table 2).

Obvious seasonal variations in the grain size of the channel-bed surficial sediments were observed in the Co Chien River (Table 2; Figs. 2c, d, 4a–d). In the Co Chien reach, sand content was higher and median value of grain size was larger during the flood season, whereas the maximum, minimum, and mean values of median grain size, as well as sand content, were all markedly lower during the dry season. In contrast, in the Co Chien–Cung Hau reach, mud was the dominant fraction and the average median grain size was only 53 μm during the flood season (Table 2). During the dry season, the clay content was lower than in the flood season, the sand content was higher (36.8%; Fig. 4a, c), and the average median grain size was higher (75 μm) (Table 2). In the Mekong River, a relatively high mud content was recorded during the flood season in the reach located about 135–150 km from the river mouth, but the other reaches showed only minor seasonal variations (Fig. 2c, d).

4.2. Magnetic susceptibility and magnetic mineral contents

Values of χ_{lf} and χ_{fd} showed overall increases from upstream to downstream reaches in all distributary channels (Table 3; Figs. 3b–c, 5). The change in χ_{fd} was closely related to the change in mud content (Fig. 6a), showing high values in all channels characterized by high mud content (Fig. 3c), in agreement with the known enrichment of superparamagnetic (SP) minerals in fine-grained sediments (Dearing et al., 1996). The relationship was much more complicated between the grain size distribution of sediments and the value of χ_{lf} (Fig. 6b). χ_{lf}, which indicates the total content of ferrimagnetic minerals (Thompson and Oldfield, 1986), increased with increasing sand fraction content in some rivers, such as the Co Chien, during the flood season (Tables 2, 3). χ_{lf} was also high in some mud-dominated channels, such as the Tr reach of the Bassac River during the dry season, but was low in the mud-dominated D-A reach (Fig. 5a).

Clear seasonal variations were observed in the magnetic susceptibility of the channel-bed surficial sediments in the Mekong–Co Chien River (Table 3; Fig. 5c, d). In the lower reach of the Mekong River (i.e., from b3 to a location about 155 km from the river mouth), values of χ_{lf} were mostly higher during the flood season than during the dry season (Fig. 5c). In addition, two reaches (at 130–150 km and ~100 km from the river mouth, respectively) were characterized by peak values of χ_{fd} during the flood season, which coincided with the peak values of mud content (Figs. 2c, 5d). Therefore, the mean values of χ_{lf} and χ_{fd} of the channel-bed surficial sediments in the Mekong River were both higher during the flood season than during the dry season (Table 3). Values of χ_{lf} in the Co Chien reach were also mostly higher, with a markedly higher mean value during the flood season compared with the dry season (Figs. 4e, 5c; Table 3). However, the values of χ_{fd} fluctuated from 0.8% to 7.3%, and the three peak values corresponded with high mud contents during the flood season (Figs. 2c, 5d), although the mean value of χ_{fd} in the Co Chien reach was similar for the flood and dry seasons (Table 3; Fig. 4f). In the Co Chien–Cung Hau reach of the Co Chien River, the mean values of both χ_{lf} and χ_{fd} were higher during the flood season (Table 3; Fig. 4e, f). In particular, substantially higher values of χ_{fd} (4.7% on average) occurred in the Co Chien–Cung Hau reach during the flood season, compared with the all distributary channels (Ham Luong, My Tho, etc.) of the Mekong River during the dry season (Figs. 4f, 5d).

4.3. Content and composition of organic carbon

TOC contents in all distributary channels generally varied in tandem with mud contents and increased downstream (Table 4; Figs. 3d, 4g, 6c, 7a, d, g, j). The relationship between the C/N ratio and grain size was quite complicated (Figs. 3e, 6d). Furthermore, the C/N ratio demonstrated clear spatial and seasonal variations in the mud-dominant reaches (Figs. 4h, 7b, e). For instance, in the two mud-dominant reaches of the Bassac River during the dry season, the C/N ratio was lower in the D-A reach than in the Tr reach (Table 4; Figs. 7b, 8a). Lower values of C/N also occurred in the downstream reaches close to the river mouths of the Co Chien–Cung Hau, Ham Luong, Cua Tieu, and Cua Dai rivers, while sediments were mud dominated there during the dry season (Figs. 4h, 7e, h, k). During the dry season, the mean C/N ratio was slightly lower in the Co Chien–Cung Hau reach than in the Co Chien reach, whereas a higher mud content was measured in the Co Chien–Cung Hau reach (Tables 2, 4). In contrast, during the flood season, the C/N ratio increased downstream along the Mekong–Co Chien–Cung Hau channels and was consistently high in the Co

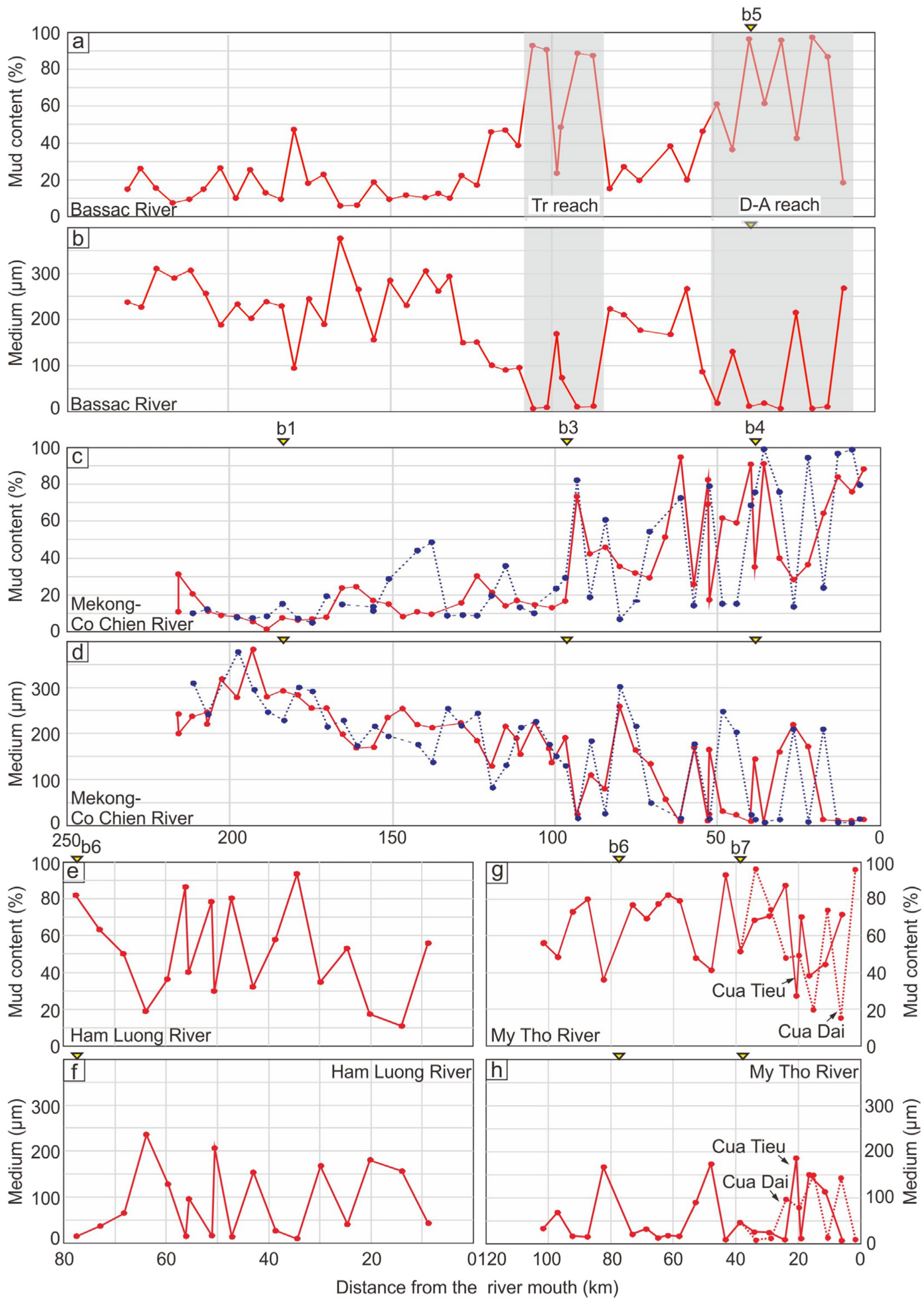

Fig. 2. Trends of sediment grain size including mud content and median grain size along distributary channels in the Mekong Delta (dry season in red, flood season in blue). The bifurcation points (b1–b7; Fig. 1B) are indicated by triangles. (a–b) The Bassac River. The shaded area represents the mud-dominated reach. (c–d) The Mekong–Co Chien–Cung Hau River. (e–f) The Ham Luong River. (g–h) The My Tho (upstream of b7), Cua Tieu (downstream of b7), and Cua Dai (dotted lines) rivers. (For interpretation of the references to colour in this figure legend, the reader is referred to the web version of this article.)

Chien–Cung Hau reach where the highest mud contents occurred (Figs. 4h, 7e, 8b).

$\delta^{13}C$ values ranging mostly from −28‰ to −26‰ for the channel-bed surficial sediments were recorded in the study area during both the flood and dry seasons (Table 4; Figs. 7, 8), reflecting a dominant terrestrial contribution (Meyers, 1994; Lamb et al., 2006). However, during the dry season, relatively enriched $\delta^{13}C$ values occurred in the lower reaches (i.e., within 60 km of the river mouth) of the Bassac–Dinh An, Co Chien–Cung Hau, Cua Dai, and Cua Tieu rivers (Table 4; Figs. 4i, 7c, f, l). During the flood season, $\delta^{13}C$ values were also more enriched in the Co Chien–Cung Hau reach than in the Co Chien reach (Table 4; Figs. 4i, 7f, 8b).

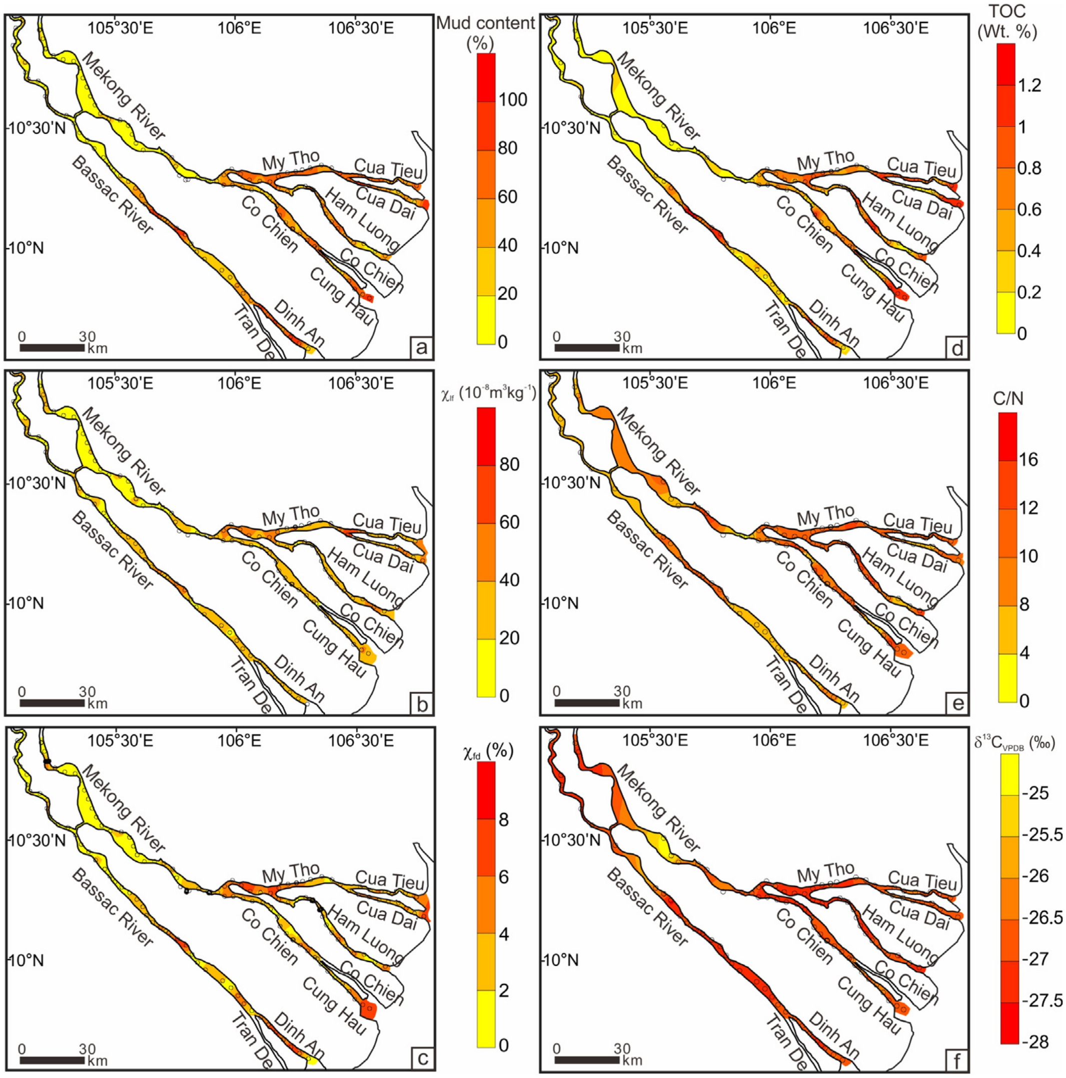

Fig. 3. Spatial distributions of (a) mud content, (b) magnetic susceptibility (χ_{lf}), (c) frequency-dependent magnetic susceptibility (χ_{fd}), (d) TOC content, (e) C/N ratio, and (f) organic carbon stable isotope $\delta^{13}C$ values along the distributary channels of the Mekong Delta during the dry season.

Seasonal differences also occurred in the content and composition of organic carbon, although terrestrial organic carbon prevailed during both the flood and dry seasons (Fig. 8). TOC contents in the Mekong River and the Co Chien–Cung Hau reach were higher during the flood season than during the dry season, but this trend was reversed in the Co Chien reach. Higher C/N ratios and more negative $\delta^{13}C$ values occurred in the Mekong–Co Chien–Cung Hau channels during the flood season compared with the dry season (Table 4). The seasonal variations in C/N ratio were most pronounced in the Co Chien–Cung Hau reach, whereas the seasonal variations in $\delta^{13}C$ values were greatest in the Mekong River (Figs. 4h, i, 7e, f).

5. Discussion

5.1. Spatial distribution of grain size and implications for sediment trapping

Results of the grain size analysis show that during both the flood and dry seasons, sandy sediments occurred mainly in the upper reaches of the Mekong and Bassac rivers (i.e., upstream of about 100–110 km from the river mouth), whereas muddy sediments prevailed in the downstream reaches (Fig. 2). This spatial variability is consistent with the recognition of fluvial- and tide-dominated regimes in the distributary channels of the Mekong Delta (Gugliotta et al., 2017) and is also consistent with the general facies pattern in the fluvial–marine transition zone of tide-dominated depositional systems (Dalrymple and Choi, 2007).

We also consider that the observed spatial distribution of grain size reflects trapping of suspended sediments in the distributary channels of the Mekong Delta, including the occurrence of the estuarine turbidity maximum; i.e., the convergence of suspended sediments supplied from the river and tidal currents therein (Fig. 9; Burchard et al., 2018). The location of the convergence zone changed seasonally in the Mekong–Co Chien–Cung Hau channels, as inferred from the seasonal variations in grain size (Fig. 2). During the dry season, the major center of mud deposition was located in the Co Chien reach (upstream of b4), whereas during the flood season it was located in the Co Chien–Cung Hau reach (downstream of b4). This seasonal migration of mud convergence is similar to the seasonal displacement of the estuarine turbidity maximum observed in other river mouths such as that of the Amazon (Asp et al., 2018). Such mud trapping in the Co Chien–Cung Hau reach of the Co Chien River during the flood season, which was probably induced by the low volume of freshwater discharge in the Co Chien River, contrasts with the process of mud export to the delta front by the Bassac–Dinh An River reported by previous studies (Wolanski et al., 1996; Nowacki et al., 2015; McLachlan et al., 2017; Ogston et al., 2017b). During the dry season in the Bassac River, two separate mud deposition centers

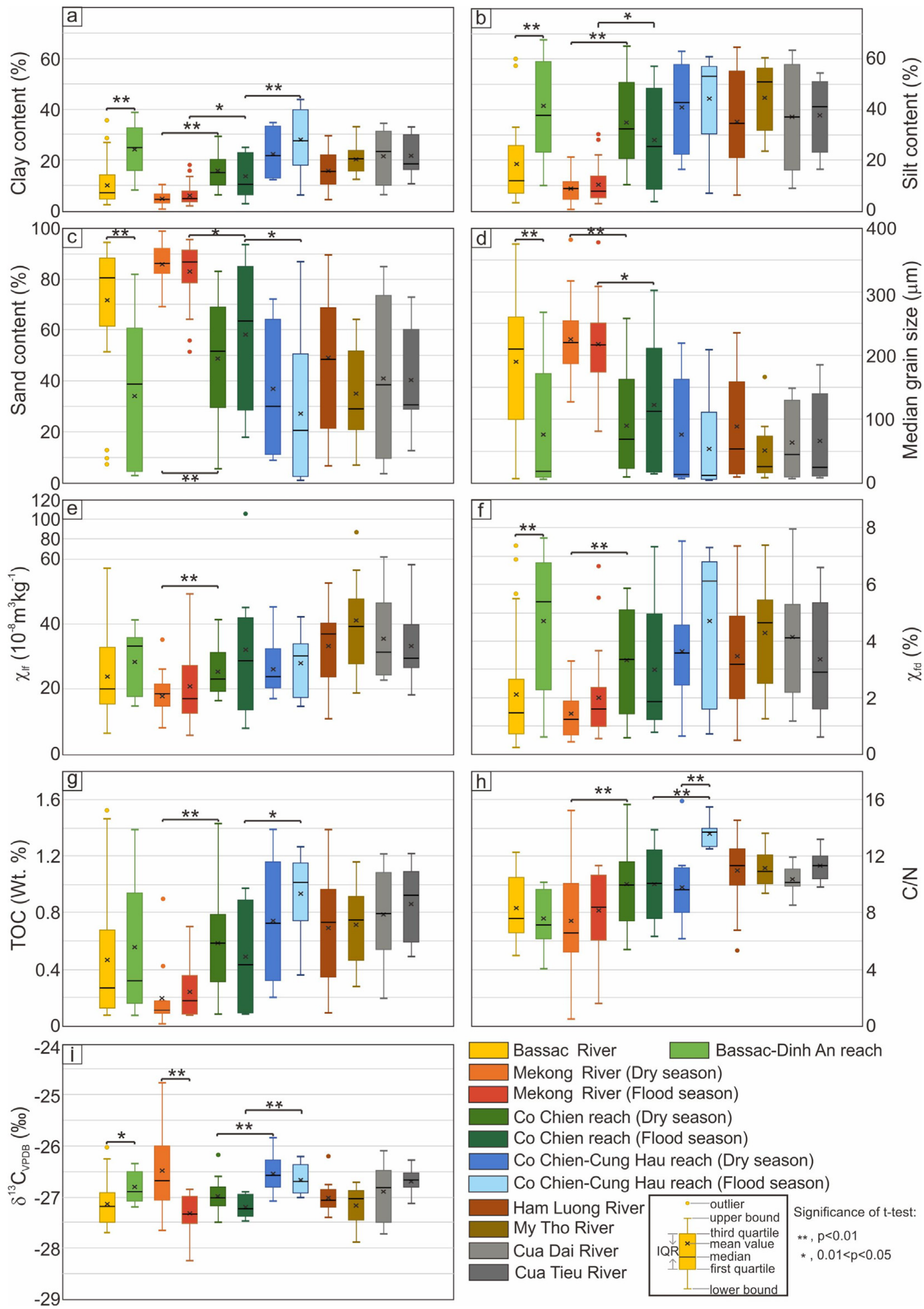

Fig. 4. Box-and-whisker plots for all measures of grain size (a–d), magnetic susceptibilities (e, f), TOC content (g), and organic elemental and isotopic compositions (h, i) for spatial and seasonal differences in channel-bed surficial sediments in the Bassac River, Mekong River, and distributary channels bifurcated from the Mekong River during the dry and flood seasons. Very significant ($p < .01$) and significant ($0.01 < p < .05$) differences between data groups as measured by *t*-tests are indicated by ** and *, respectively.

indicate a zone of mud convergence in the freshwater reach and another close to the river mouth (Figs. 2a, 9). The hydro-sedimentary dynamic processes controlling the described seasonal and spatial variations in mud convergence are discussed below with respect to sediment source discrimination (Table 5).

5.2. Seasonal and spatial variations in sediment sources

There are two major sources (i.e., riverine and marine) of the fine-grained sediments trapped in the distributary channels of the Mekong Delta, as inferred from their magnetic susceptibilities (χ_{lf} and χ_{fd}) and organic geochemical compositions (Figs. 5, 7; Table 5). Values of χ_{lf}

Table 2
Statistics for sediment grain-size composition and median grain size for channel-bed surficial sediments collected from the Mekong–Co Chien River during the flood season and all distributary channels during the dry season. Italicized text represents sand-dominated reaches, and bolded text represents the finest grain size during the flood and dry seasons, respectively. The Co Chien reach corresponds to the river tract between b3 and b4 and the Co Chien–Cung Hau reach corresponds to the river tract downstream of b4 (Fig. 1B). The Bassac–Din An reach corresponds to the river tract downstream of b5.

Sampling season	River reach	Number of samples	Clay (%)		Silt (%)		Sand (%)		Median grain size (μm)	
			Range	Mean	Range	Mean	Range	Mean	Range	Mean
Dry season	*Bassac*	*39*	*2.3–35.5*	*9.8*	*3.4–61.4*	*18.6*	*7.2–94.3*	*71.6*	*6.9–375.0*	*189.7*
	Bassac–Dinh An	9	8.1–38.7	24.5	10.1–67.7	41.5	2.9–81.8	34.0	6.0–267.6	75.9
	Mekong	*30*	*0.5–10.4*	*5.0*	*0.6–21.3*	*9.0*	*69.1–98.9*	*86.0*	*128.0–381.4*	*224.8*
	Co Chien	14	6.2–29.3	16.1	10.7–65.2	35.1	5.5–83.1	48.8	9.3–258.2	89.8
	Co Chien–Cung Hau	10	11.3–34.7	22.2	16.7–63.1	41.0	8.9–72.0	36.8	6.7–218.5	75.4
	Ham Luong	18	4.2–29.4	15.7	6.5–64.6	35.2	6.7–89.3	49.1	9.0–235.1	88.5
	My Tho	**14**	**12.3–33.1**	**20.4**	**23.5–60.4**	**44.6**	**7.0–64.2**	**35.0**	**8.3–173.2**	**50.9**
	Cua Dai	8	6.1–34.4	21.8	9.0–63.7	37.1	3.7–84.9	41.1	7.2–148.9	63.0
	Cua Tieu	8	10.5–33.0	21.7	16.7–54.4	38.0	12.6–72.8	40.3	7.9–185.7	66.0
Flood season	*Mekong*	*25*	*1.8–17.9*	*6.3*	*2.9–30.6*	*10.6*	*51.5–95.3*	*83.2*	*81.5–377.6*	*217.7*
	Co Chien	***12***	***2.7–24.9***	***13.7***	***3.8–57.2***	***28.1***	***17.9–93.5***	***58.2***	***14.0–301.4***	***122.2***
	Co Chien–Cung Hau	9	6.1–43.9	28.3	7.1–61.1	44.5	1.0–86.8	27.2	4.8–209.0	53.3

Table 3
Range and mean values of χ_{lf} and χ_{fd} (%) for the Mekong–Co Chien River during the flood season and all distributary channels during the dry season.

Sampling season	River reach	Number of samples	χ_{lf} ($10^{-8}m^3kg^{-1}$)		χ_{fd} (%)	
			Range	Mean	Range	Mean
Dry season	Bassac	39	6.4–57.2	24.0	0.2–7.4	2.1
	Bassac–Dinh An	9	14.9–41.3	28.5	0.6–7.7	4.7
	Mekong	31	7.8–34.7	17.8	0.5–3.3	1.4
	Co Chien	14	16.3–41.1	25.6	0.6–5.9	3.3
	Co Chien–Cung Hau	10	16.9–45.4	26.2	0.6–7.5	3.6
	Ham Luong	18	10.6–52.4	33.5	0.5–7.4	3.5
	My Tho	15	18.3–86.8	41.2	1.3–7.4	4.3
	Cua Dai	8	22.4–61.3	35.6	1.2–8.0	4.1
	Cua Tieu	8	17.8–58.3	33.4	0.6–6.6	3.4
Flood season	Mekong	25	5.8–49.1	20.8	0.6–7.1	2.0
	Co Chien	13	8.2–105.3	32.2	0.8–7.3	3.0
	Co Chien–Cung Hau	9	15.0–41.9	28.0	0.7–7.3	4.7

reflect the content of ferrimagnetic minerals, which are derived predominantly from bedrock, whereas values of χ_{fd} reflect the content of superparamagnetic (SP) grains, which are enriched in soil (Thompson and Oldfield, 1986; Oldfield et al., 2003; Oldfield and Crowther, 2007). Thus, riverine sediments are characterized by high values of magnetic susceptibilities because they are derived from bedrock and soil erosion in the drainage basin (Thompson and Oldfield, 1986). Dissolution of detrital magnetic minerals, including SP grains, generally occurs as a result of early diagenesis after burial in sediments, leading to a reduction in magnetic susceptibility (Karlin and Levi, 1983; Snowball, 1993; Evans et al., 1997; Robinson et al., 2000). In addition, it was reported that deposits in the river mouth of the Yangtze over the last few hundred years have been characterized by higher values of magnetic susceptibility compared with older sediments because of the intensified rock and soil erosion induced by the increase in human population in the drainage basin (Wang et al., 2011a; Pan et al., 2017). Thus, we infer lower values of magnetic susceptibility for resuspended or reworked fine-grained sediments derived from a marine source than for suspended sediments newly supplied from the drainage basin, because of either early diagenesis or less intense human activity in an earlier period (Ge et al., 2017). Organic geochemical compositions can also help identify a marine source because marine algae or particulate organic carbon (POC) is characterized by lower C/N ratios and more enriched $\delta^{13}C$ values than other sources (Meyers, 1997; Lamb et al., 2006). Early diagenesis can also reduce C/N ratios and increase values of $\delta^{13}C$ (Meyers, 1997; Kohzu et al., 2011). Thus, both marine-derived and reworked sediments should have lower C/N ratios and enriched $\delta^{13}C$ values. By combining data for magnetic susceptibilities, C/N, and $\delta^{13}C$, we are able to identify spatial and temporal patterns of the riverine or marine source of the studied channel-bed surficial sediments (Table 5). In the discussion below, we focus on the direction of change, rather than absolute values, because we were unable to accurately collect the sediments deposited in a single flood or dry season during the sampling.

We speculate that the newly deposited sediments along the Mekong–Co Chien–Cung Hau channels during the flood season were supplied mostly from the drainage basin, as inferred from the high values of magnetic susceptibilities and C/N ratios and the depleted $\delta^{13}C$ values of the channel-bed surficial sediments (Fig. 4; Table 5). Spatial patterns of these newly deposited sediments included an increase in the sand fraction of the Co Chien reach and in the mud fraction of the Co Chien–Cung Hau reach compared with the dry season (Table 2). Mud in the Co Chien–Cung Hau reach showed more enriched $\delta^{13}C$ values compared with upstream reaches (Table 4; Fig. 4), indicating a contribution from marine algae and/or marine POC in addition to the major contribution from the drainage basin.

During the dry season, the higher mud content in the Co Chien reach was characterized by only a small increase in the χ_{fd} value compared with the flood-season samples, which indicates that the mud was derived from buried sediments, as SP grains are typically dissolved first during early diagenesis (Karlin and Levi, 1983). Furthermore, the lower C/N ratios and less negative $\delta^{13}C$ values of this mud (Table 4; Fig. 4) constitute a signature of marine algae and/or POC (Meyers, 1994; Lamb et al., 2006) or of early diagenesis (Meyers, 1997; Kohzu et al., 2011). The possible early diagenesis signal indicates that the mud was derived from resuspended sediments that had previously been deposited elsewhere. Similarly, the content of ferrimagnetic minerals in the Co Chien–Cung Hau reach was lower despite the higher sand content during the dry season compared with the flood season (Tables 3, 5; Fig. 4e, f), which also indicates early diagenesis (Karlin and Levi, 1983) and agrees with the reported presence of recycled sand there (Gugliotta et al., 2017). Early diagenesis of organic carbon or a contribution from marine algae and/or POC is also inferred from the lower C/N ratios and enriched $\delta^{13}C$ values in the Co Chien–Cung Hau reach during the dry season compared with the flood season (Table 5; Fig. 4h, i), with the enriched $\delta^{13}C$ being consistent with the dominant marine and brackish water species of the diatoms at that location (Gugliotta et al., 2017). Lower magnetic susceptibilities and less negative $\delta^{13}C$ values also

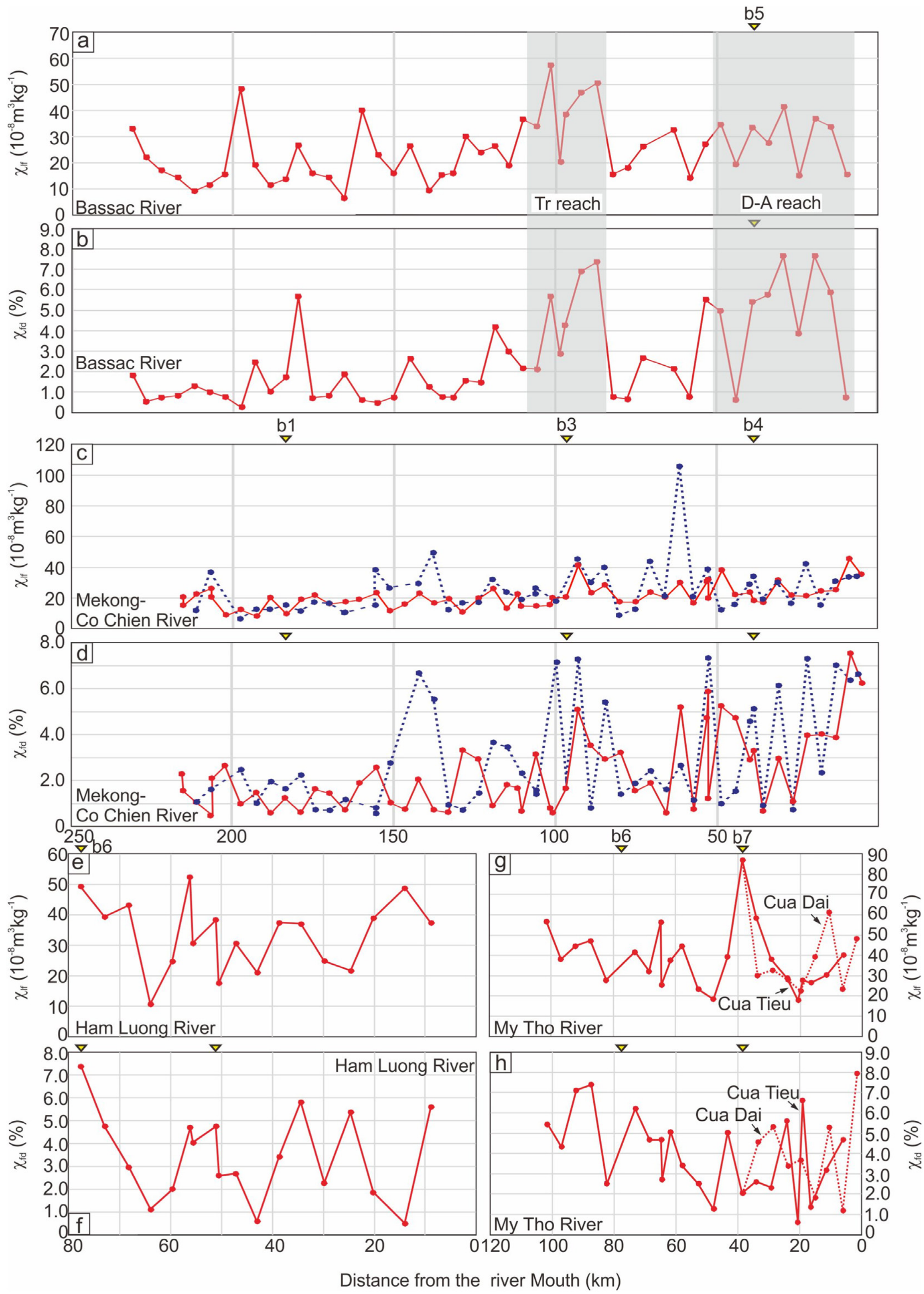

Fig. 5. Trends of magnetic susceptibility (χ_{lf}) and frequency-dependent magnetic susceptibility (χ_{fd}) along distributary channels in the Mekong Delta (dry season in red, flood season in blue). Information for the shaded areas and channel names is the same as that given in Fig. 2. (For interpretation of the references to colour in this figure legend, the reader is referred to the web version of this article.)

occurred in the Mekong River during the dry season, suggesting a possible contribution from C_4 plants such as sugar cane and corn, or the early diagenesis of sediments, or a contribution by marine-sourced organic carbon. However, the low C/N ratios do not support a contribution from C_4 plants (Fig. 4). The intensive in-channel extraction of bed aggregate in the Mekong River during the low-flow season (Brunier et al., 2014) has removed recent deposits and exposed old deposits in the channel bed. As such, early diagenesis may better explain the enriched $\delta^{13}C$ values, supported by the lower magnetic susceptibility. Sand mining could also expose former marine-influenced sediments to the channel bed, leading to the enriched $\delta^{13}C$ values. Thus, signatures of reworked or marine-sourced sediments occurred in the surficial sediments in the Mekong–Co Chien–Cung Hau channels during the dry season.

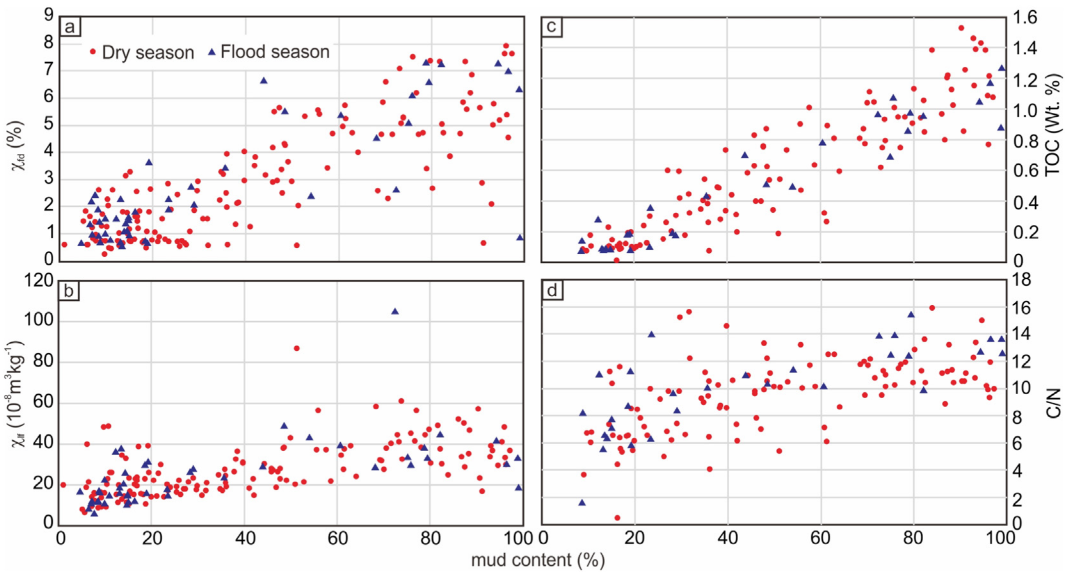

Fig. 6. Correlation between mud content and (a) frequency-dependent magnetic susceptibility (χ_{fd}), (b) magnetic susceptibility (χ_{lf}), (c) TOC content, and (d) C/N ratio for all samples during the dry and flood seasons.

Although no sediments were collected during the flood season from other distributary channels of the Mekong River, including the Ham Luong, My Tho, Cua Dai, and Cua Tieu rivers, the lower values of χ_{fd} and C/N of the muds in these channels during the dry season compared with the Co Chien–Cung Hau reach during the flood season (Fig. 4f, h) suggest that signatures of resuspended sediments and a marine influence also occurred in these channels during the dry season.

The two mud deposition centers (Tr and D-A reaches) in the Bassac River during the dry season have different sediment sources, as inferred from their differing magnetic properties and organic geochemical compositions (Table 5). Similar to the mud deposits close to the Cung Hau mouth of the Co Chien River during the flood season, the higher values of magnetic susceptibility (Fig. 5a) and C/N ratios and the depleted $\delta^{13}C$ values (Fig. 7b, c) indicate a riverine source of mud in the Tr reach of the Bassac River deposited during the dry season. In contrast, the mud in the D-A reach close to the Bassac River mouth shows signatures of early diagenesis and marine algae and/or POC (Table 5).

5.3. Seasonal and spatial variations in hydro-sedimentary dynamic processes

Sediment trapping occurred in the Mekong–Co Chien River during both the dry and flood seasons. This pattern differs from the seasonal variations in the Bassac–Dinh An River, which are characterized by mud export to the coast and sea during the flood season and mud import from the coast and subaqueous delta during the dry season (Wolanski et al., 1996; Wolanski et al., 1998; Kanai et al., 2013a, 2013b; Nowacki et al., 2015; McLachlan et al., 2017). We explain this difference in terms of hydro-sedimentary processes. First, the trapping of suspended sediment in the Mekong–Co Chien River during the flood season reflects weaker freshwater flow and stronger salinity intrusion than in the Bassac–Dinh An River. Second, the seasonal differences in sediment delivery to the Mekong–Co Chien River discussed in Section 5.2 are indicative of variations in sediment transport processes in the tidal-river and estuarine regimes during the flood and dry seasons (Fig. 9a, b).

The magnetic mineral and organic carbon compositions of the channel-bed surficial sediments reflect the riverine sediment supply in the Co Chien River during the flood season (Table 5). This deposition of newly supplied riverine sediments implies trapping of fluvial sediments in the distributary channels induced by the saltwater wedge and tidal processes (Fig. 9a) rather than export to the delta front as in the case of the Bassac–Dinh An River (Kanai et al., 2013a, 2013b). We explain this difference in terms of the following. First, saltwater intrusion occurred within ~15 km of the Cung Hau mouth of the Co Chien River, and a highly stratified water column formed in the lowest reach (Fig. 9a; Gugliotta et al., 2017). As a result of the hindering effect of the saltwater wedge, the near-bed shear stress weakened (McLachlan et al.,

Table 4
Range and mean values of $\delta^{13}C$, C/N, and TOC for the Mekong–Co Chien River during the flood season and all distributary channels during the dry season.

Sampling season	River reach	Number of samples	$\delta^{13}C$ (‰)		C/N		TOC (wt%)	
			Range	Mean	Range	Mean	Range	Mean
Dry season	Bassac	23	−27.70 to −26.02	−27.13	5.0–12.3	8.3	0.07–1.53	0.46
	Bassac–Dinh An	9	−27.19 to −26.35	−26.70	4.1–10.2	7.6	0.08–1.39	0.56
	Mekong	13	−27.66 to −24.76	−26.47	0.5–15.3	7.5	0.01–0.90	0.19
	Co Chien	14	−27.50 to −26.16	−26.53	5.4–15.7	10.0	0.08–1.43	0.58
	Co Chien–Cung Hau	10	−27.08 to −25.85	−26.53	6.2–15.9	9.8	0.20–1.39	0.74
	Ham Luong	17	−27.39 to −26.21	−27.00	5.3–14.6	11.0	0.09–1.39	0.69
	My Tho	14	−27.88 to −26.71	−27.16	9.4–13.7	11.2	0.28–1.16	0.72
	Cua Dai	7	−27.72 to −26.10	−26.89	8.5–12.0	10.4	0.20–1.22	0.79
	Cua Tieu	8	−27.14 to −26.28	−26.68	9.8–13.2	11.3	0.49–1.22	0.86
Flood season	Mekong	13	−28.25 to −26.63	−27.32	1.6–11.3	8.2	0.08–0.82	0.24
	Co Chien	10	−27.46 to −26.90	−27.18	6.4–13.9	10.1	0.08–0.97	0.49
	Co Chien–Cung Hau	8	−27.00 to −26.20	−26.66	12.5–15.5	13.6	0.36–1.27	0.94

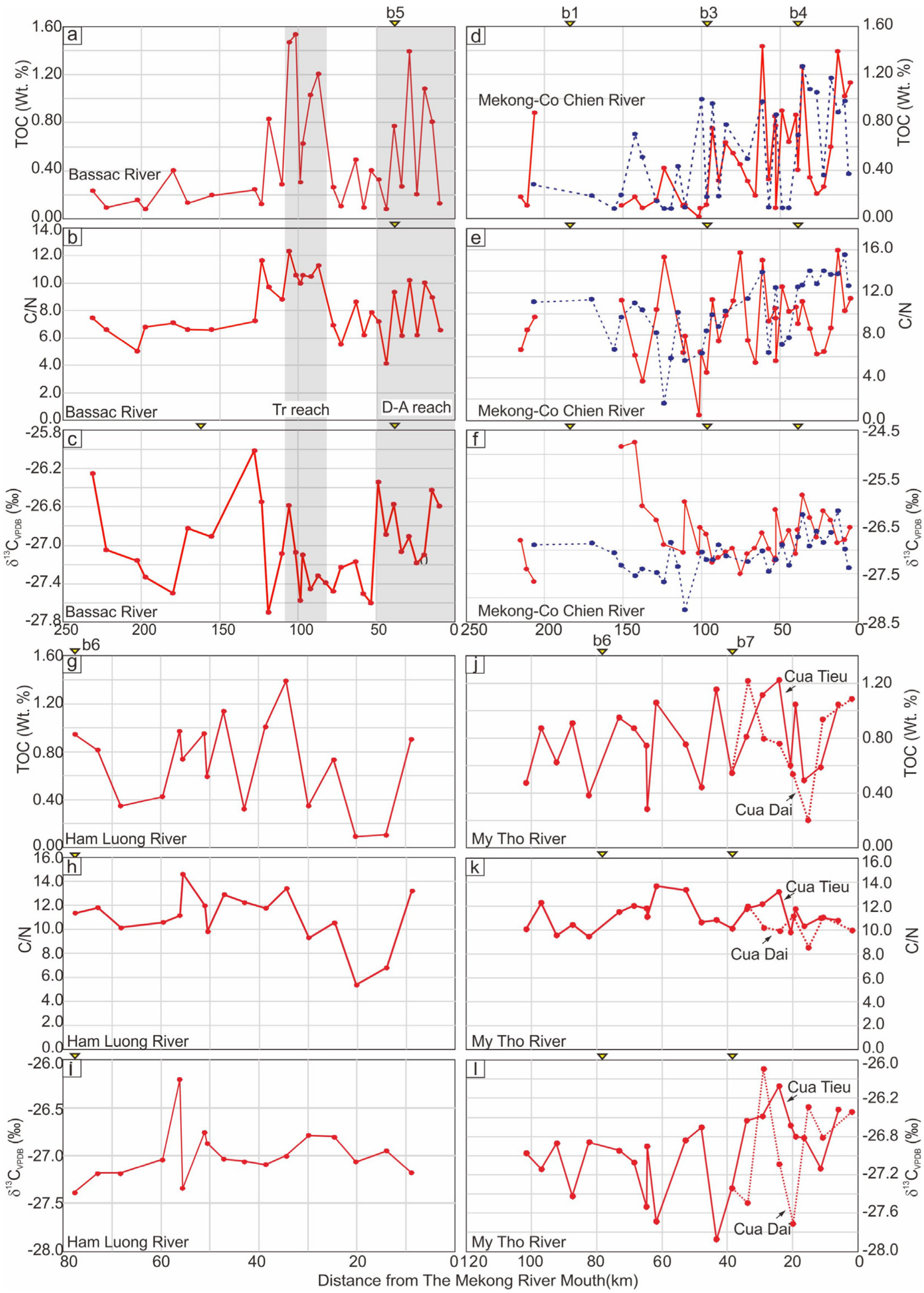

Fig. 7. Trends of TOC content, C/N ratio, and $\delta^{13}C$ values along distributary channels in the Mekong Delta (dry season in red, flood season in blue). (a–c) The Bassac River. Shaded areas represent the mud-dominated reaches as indicated in Fig. 2. (d–f) The Mekong–Co Chien–Cung Hau River. (g–i) The Ham Luong River. (j–l) The My Tho (upstream of b7), Cua Tieu (downstream of b7), and Cua Dai (dotted lines) rivers. (For interpretation of the references to colour in this figure legend, the reader is referred to the web version of this article.)

2017) in the lower reach of the freshwater-dominated river and resulted firstly in the deposition of the sand fraction from the suspended sediments in the Co Chien reach and then the deposition of mud in the Co Chien–Cung Hau reach (Table 2). Although the saltwater intrusion extended only ~15 km upstream of the river mouth, deposition of the suspended sediments went far beyond this range, possibly because of the occurrence of an interface zone between the tidal-river and estuarine regimes, as proposed by McLachlan et al. (2017). In addition, estuarine circulation caused by the saltwater wedge also promoted mud deposition at the toe of the salt wedge; i.e., in the lower reach close to the Cung Hau River mouth (Fig. 9a). Second, we suggest that the bifurcations (b3 and b4; Fig. 1B) and associated reduction in freshwater discharge led to a weakening in the river flow and higher ratio between the tidal prism and water volume of the freshwater discharge in the Co

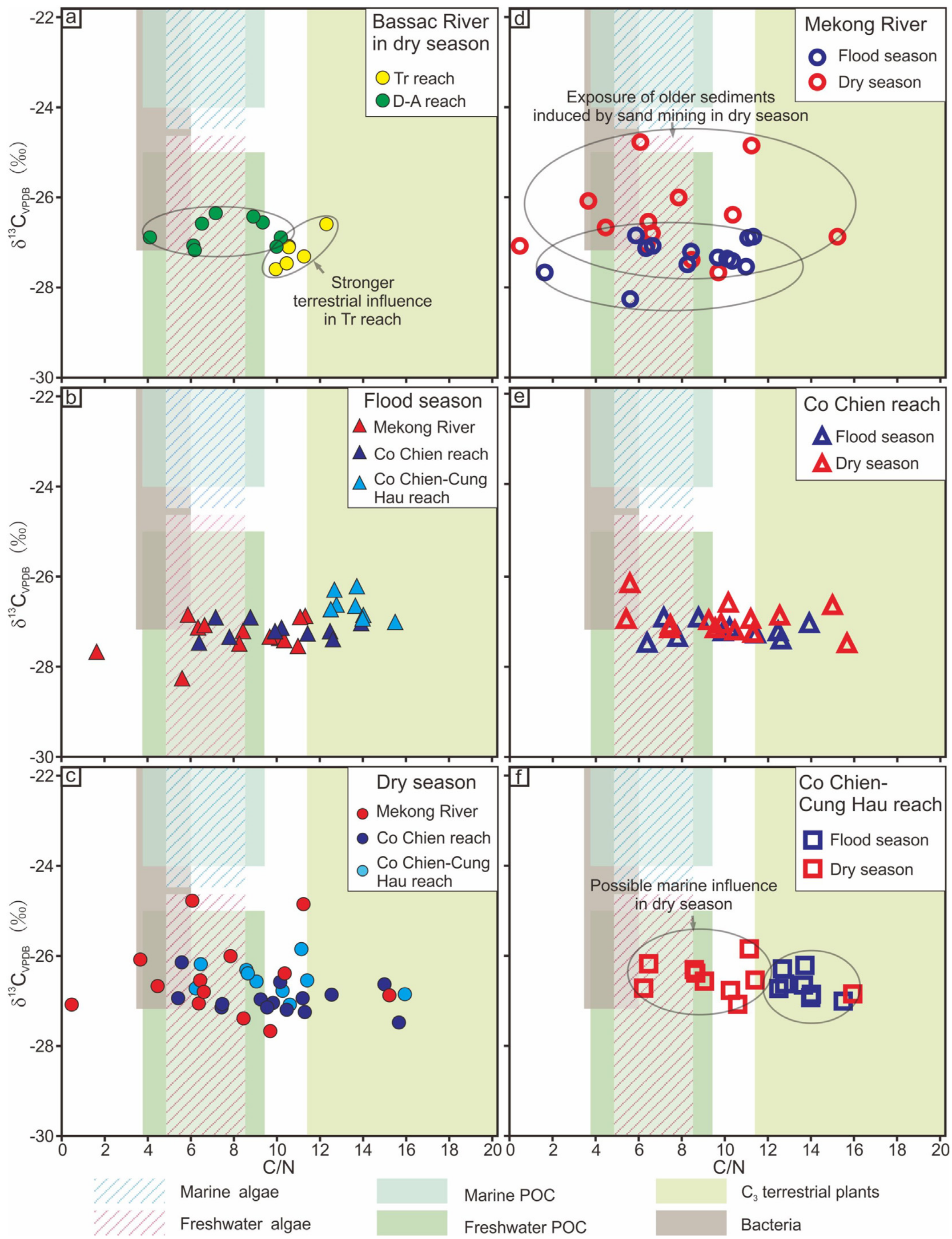

Fig. 8. Plots of C/N vs. δ^{13}C for channel-bed surficial samples in the two mud-dominated reaches (Tr and D-A) in the Bassac River during the dry season (a) and channel-bed surficial samples in the Mekong–Co Chien–Cung Hau River during the flood and dry seasons (b–f). Regions for the different types of organic matter are after Lamb et al. (2006).

Chien–Cung Hau reach compared with the Bassac–Dinh An River (Fig. 9a), which favored preservation of the mud deposited during slack tides.

The signal of marine algae and/or POC in the channel-bed surficial sediments of the Co Chien–Cung Hau reach during the flood season (Table 5) further indicates the occurrence of estuarine circulation or tidal pumping, which transported the marine algae and/or POC from the estuary or continental shelf into the Co Chien–Cung Hau reach. Therefore, unlike the intermittent appearance at Dinh An, we speculate the presence of a persistent saltwater intrusion in the Co Chien–Cung Hau reach even during the flood season; this persistent intrusion plays an important role in the trapping of riverine suspended sediments in the distributary channel of the Mekong River.

During the dry season, the saltwater intrusion extended as far as the Co Chien reach, and fine-grained sediments were deposited there as a result of tidal pumping and estuarine circulation (Fig. 9b). Because of the low dry-season freshwater discharge, the flood tide prevailed, leading to strong tidal pumping in the Co Chien River during the dry season. Unlike the riverine supply of sediment during the flood season, we suggest that mud deposited in the Co Chien reach during the dry season was imported primarily from resuspended sediments from the downstream reach, delta front and offshore areas, (Fig. 9b) as indicated

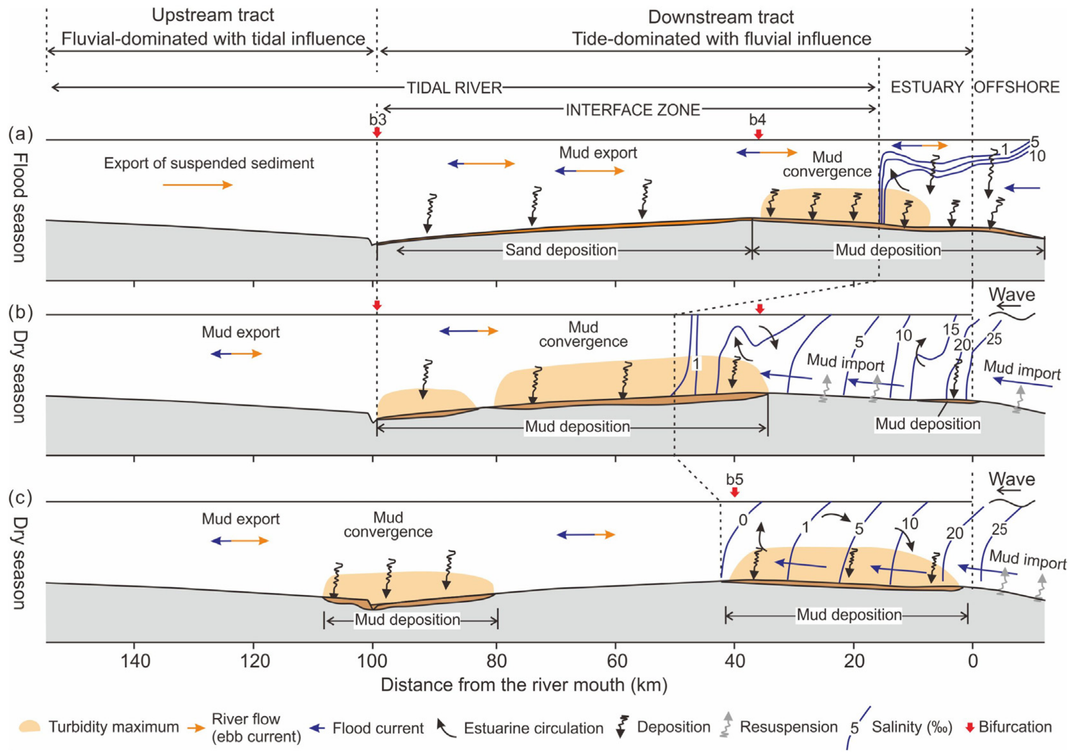

Fig. 9. Conceptual model of depositional processes in the Mekong–Co Chien–Cung Hau River during (a) the flood season and (b) the dry season and (c) in the Bassac–Dinh An River during the dry season. Mud convergence occurred in the interface zone between the tidal river and estuary and in the saltwater wedge as suggested by previous studies in the Mekong–Co Chien–Cung Hau River during both the flood (a) and dry (b) seasons (Wolanski et al., 1996; McLachlan et al., 2017). In contrast, two mud convergence zones occurred in the Bassac–Dinh An River during the dry season: one in the freshwater region and the other in the saltwater wedge (c).

by signals of early diagenesis or marine algae and/or POC (Table 5). We speculate that resuspension and upstream transportation of mud deposited during an earlier flood season occurred in the Co Chien–Cung Hau reach during the dry season, on the basis of the coarsening of surficial sediments there (Table 2; Fig. 4), which could have been caused by strong tidal currents during the dry season (Fig. 9b; Gugliotta et al., 2017). Such processes might explain the recycled sand in the Co Chien–Cung Hau reach during the dry season reported by Gugliotta et al. (2017). Another possible origin of the coarser surficial sediments characterized by early diagenesis in the Co Chien–Cung Hau reach during the dry season (Table 5) is the sand mining, which has generally taken place during low flow (Bravard et al., 2013). However, Brunier et al. (2014) suggested that less sand mining occurred in the distributary channels bifurcated from the Mekong River compared with the Bassac River, possibly because of the dominant mud deposition in the distributary channels of the Mekong River as indicated by the present results (Fig. 2). In addition, the marine algae and/or POC in the Co Chien–Cung Hau reach during the dry season could have been transported from the offshore area or produced in situ by a predominant estuarine regime.

During the dry season, the muddy deposits in the Bassac River were characterized by early diagenesis and a marine source of organic carbon in the lower reach (the D-A reach; Fig. 2a) close to the Dinh An mouth, possibly reflecting mud import from the coastal zone and delta front by tidal pumping and estuarine circulation (Wolanski et al., 1996; Wolanski et al., 1998; Kanai et al., 2013a, 2013b; Nowacki et al., 2015; McLachlan et al., 2017; Fig. 9c). The other mud depocenter in the freshwater region of the Bassac River (the Tr reach) had a riverine sediment source, as inferred from magnetic properties and organic elemental composition (Table 5). Therefore, two separate turbidity maxima were present in the Bassac River during the dry season, in contrast to the pattern in the Mekong–Co Chien River in the same season and also to the interface zone between the tidal river and estuary proposed by previous studies (McLachlan et al., 2017; Ogston et al., 2017b). The turbidity maximum close to the river mouth (D-A reach) occurred within the region of the salinity intrusion (Fig. 9c), which is consistent with being generated by estuarine circulation (Wolanski et al., 1996; Wolanski et al., 1998; Burchard et al., 2018). There seems to be no mud deposition in the interface zone; i.e., the reach several kilometers upstream of the salinity intrusion (McLachlan et al., 2017). Tidal asymmetry could be a major mechanism for mud deposition in the Tr reach (Burchard et al., 2018), as this reach is located in the transition zone from a fluvial- to tide-dominated regime (Gugliotta et al., 2017). Similar mud deposition patterns have been observed in the transition zone of the Yangtze River mouth (Wang et al., 2009; Gugliotta and Saito, 2019). An alternative mechanism might be intensive channel incision induced by sanding mining, which has been stronger in the Bassac River than in the Mekong–Co Chien River (Brunier et al., 2014). We suggest that further field observations are necessary to better understand the mud depocenters in the Bassac River in dry season.

6. Conclusions

This study analyzed spatial and seasonal variations in the properties of channel-bed surficial sediments in distributary channels of the Mekong Delta. We draw the following conclusions about the sedimentary record and associated dynamic processes.

1. The spatial distribution of sediments is characterized by coarse-grained sediment in upstream reaches and fine-grained sediment in downstream reaches during both flood and dry seasons. This is consistent with the fluvial- and tide-dominated regimes of the Mekong Delta plain.
2. Seasonal variations were observed in the magnetic minerals and

Table 5
Comparison of channel-bed surficial sediment characteristics between flood and dry seasons in the Mekong–Co Chien River and between the two mud-dominated reaches (Tr and D-A) in the Bassac River during the dry season.

Sampling season	Sampling location	Sediment composition	Magnetic susceptibilities and content of magnetic minerals	TOC content	C/N ratios, $\delta^{13}C$ values, and OC source
Flood season	Mekong River	Some increase in mud deposition in the lower reach	Slight increase in both χ_{lf} and χ_{fd}, reflecting increase in contents of ferrimagnetic and SP minerals	Slight increase	Higher C/N ratios and depleted $\delta^{13}C$ values, indicating terrestrial C_3 plants
	Co Chien reach	Higher sand content	Obvious increase in χ_{lf}, indicating higher content of ferrimagnetic minerals	Decrease	Higher C/N ratios and depleted $\delta^{13}C$ values, indicating terrestrial C_3 plants
	Co Chien–Cung Hau reach	Higher mud content	Increase in both χ_{lf} and χ_{fd}, indicating higher contents of both ferrimagnetic and SP minerals	Obvious increase	Highest C/N ratios reflecting dominant terrestrial C_3 plants. Slightly enriched $\delta^{13}C$ values indicating some signature of marine algae/POC
Dry season	Mekong River	Slightly coarser	Lower values of both χ_{lf} and χ_{fd}; lower content of magnetic minerals	Slight decrease	Lower C/N ratios and enriched $\delta^{13}C$ values, indicating degraded terrestrial C_3 plants
	Co Chien reach	Higher mud content	Lower values of χ_{lf} and weak increase in χ_{fd}; little increase in the SP grains, indicating early diagenesis	Increase	Lower C/N ratios and enriched $\delta^{13}C$ values, indicating additional contribution from the marine algae/POC
	Co Chien–Cung Hau reach	Higher sand content	Lower values of both χ_{lf} and χ_{fd}; lower contents of both ferrimagnetic and SP minerals, indicating early diagenesis	Decrease	Lower C/N ratios and enriched $\delta^{13}C$ values, indicating additional contribution from the marine algae/POC
Dry season	Tr reach of Bassac River	Mud-dominated	Higher values of χ_{lf}, higher content of ferrimagnetic minerals	High	High C/N ratios and depleted $\delta^{13}C$ values, indicating dominant terrestrial C_3 plants
	D-A reach of Bassac River	Mud-dominated	Lower values of χ_{lf}, lower content of ferrimagnetic minerals	High	Lower C/N ratios and enriched $\delta^{13}C$ values, indicating additional contribution from the marine algae/POC

organic carbon compositions of channel-bed surficial sediments in the Mekong–Co Chien River. Higher contents of magnetic minerals and terrestrial organic carbon occurred during the flood season compared with the dry season, reflecting trapping of fluvial-supplied suspended sediments in the distributary channel. The presence of marine algae and/or POC in the most downstream reach during the flood season suggests the occurrence of a saltwater wedge and associated estuarine circulation. During the dry season, mud deposition occurred in the Co Chien reach, characterized by early diagenesis or a contribution from marine algae and/or POC, reflecting the import of resuspended mud from the downstream channel or nearshore area.

3. During the dry season, there were two mud-dominated reaches in the Bassac River: the Tr reach and the D-A reach. The mud in the Tr reach contained higher magnetic mineral and terrestrial organic carbon contents, suggesting an origin from fluvial sediments supplied from the drainage basin. The mud in the D-A reach was characterized by early diagenesis or a signature of marine algae and/or POC, indicating an origin from resuspended sediments sourced from the nearshore area.

Declaration of competing interests

On behalf of all coauthors, I state that this study has no competing interests to declare.

Acknowledgments

This research was conducted as a part of a joint research program between Shimane University and HCMC Institute of Resources Geography, VAST. This study was supported by the National Key Research and Development Program, China (Grant No. 2016YFC0402600), the Open Research fund of the State Key Laboratory of Estuarine and Coastal Research, China (Grant No. SKLEC-PGKF201902), and a KAKENHI grant from the Japan Society for the Promotion of Science (JSPS) (Grant No. JP 17H02980). Further support was provided by the NAFOSTED Vietnam project 105.03-2018.12. The authors are grateful to the Editor and two anonymous reviewers for their constructive comments.

References

Allison, M.A., Nittrouer, C.A., Ogston, A.S., Mullarney, J.C., Nguyen, T.T., 2017a. Sedimentation and survival of the Mekong Delta: a case study of decreased sediment supply and accelerating rates of relative sea level rise. Oceanography 30 (3), 98–109.

Allison, M.A., Dallon Weathers, H., Meselhe, E.A., 2017b. Bottom morphology in the Song Hau distributary channel, Mekong River delta, Vietnam. Cont. Shelf Res. 147, 51–61.

Fluvial-tidal sedimentology. In: Ashworth, P.J., Best, J.L., Parsons, D.R. (Eds.), Developments in Sedimentology. 68. pp. 1–634.

Asp, N.E., Gomes, V.J.C., Schettini, C.A.F., Souza-Filho, P.W.M., Siegle, E., Ogston, A.S., Nittrouer, C.A., Silva, J.N.S., Nascimento Jr., W.R., Souza, S.R., Pereira, L.C.C., Queiroz, M.C., 2018. Sediment dynamics of a tropical tide-dominated estuary: Turbidity maximum, mangroves and the role of the Amazon River sediment load. Estuar. Coast. Shelf Sci. 214, 10–24.

Bravard, J.-P., Goichot, M., Gaillot, S., 2013. Geography of sand and gravel mining in the lower Mekong River. EchoGéo. https://doi.org/10.4000/echogeo.13659.

Brunier, G., Anthony, E.J., Goichot, M., Provansal, M., Dussouillez, P., 2014. Recent morphological changes in the Mekong and Bassac river channels, Mekong delta: the marked impact of river-bed mining and implications for delta destabilization. Geomorphology 224, 177–191.

Burchard, H., Schuttelaars, H.M., Ralston, D.K., 2018. Sediment trapping in estuaries. Annu. Rev. Mar. Sci. 10, 371–395.

Dalrymple, R.W., Choi, K., 2007. Morphologic and facies trends through the fluvial-marine transition in tide-dominated depositional systems: a schematic framework for environmental and sequence-stratigraphic interpretation. Earth-Sci. Rev. 81 (3–4), 135–174.

Dearing, J.A., Dann, R.J.L., Hay, K., Lees, J.A., Loveland, P.J., Maher, B.A., Grady, K.O., 1996. Frequency-dependent susceptibility measurements of environmental materials. Geophys. J. Int. 124, 228–240.

Dee, D.P., Uppala, S.M., Simmons, A.J., Berrisford, P., Poli, P., Kobayashi, S., Andrae, U., Balmaseda, M.A., Balsamo, G., Bauer, P., Bechtold, P., Beljaars, A.C.M., van de Berg, L., Bidlot, J., Bormann, N., Delsol, C., Dragani, R., Fuentes, M., Geer, A.J., Kohler, M., Matricardi, M., McNally, A.P., Monge-Sanz, B.M., Morcrette, J.J., Park, B.K., Peubey,

C., de Rosnay, P., Tavolato, C., Thepaut, J.N., Vitart, F., 2011. The ERA-Interim reanalysis: configuration and performance of the data assimilation system. Q. J. R. Meteorol. Soc. 137 (656), 553–597.
Evans, M., Heller, F., Bloemendal, J., Thouveny, N., 1997. Natural magnetic archives of past global change. Surv. Geophys. 18, 183–196.
Freitas, P.T.A., Asp, N.E., e Souza-Filho, P.W.M., Nittrouer, C.A., Ogston, A.S., da Silva, M.S., 2017. Tidal influence on the hydrodynamics and sediment entrapment in a major Amazon River tributary-lower Tapajós River. J. S. Am. Earth Sci. 79, 189–201.
Gagliano, S.M., McIntire, W.G., 1968. Reports on the Mekong River delta. In: Coastal Studies Institute Technical Report No. 57. Louisiana State University (143 p).
Gao, S., Collins, M.B., 2014. Holocene sedimentary systems on continental shelves. Mar. Geol. 352 (3), 268–294.
Ge, C., Zhang, W., Dong, C., Wang, F., Feng, H., Qu, J., Yu, L., 2017. Tracing sediment erosion in the Yangtze River subaqueous delta using magnetic methods. Journal of Geophysical Research-Earth Surface 122, 2064–2078.
Geyer, W.R., 1988. The advance of a salt wedge front: Observations and dynamical model. In: Dronkers, J., van Leussen, W. (Eds.), Physical Processes in Estuaries. Springer-Verlag, pp. 181–195.
Gugliotta, M., Saito, Y., 2019. Matching trends in channel width, sinuosity, and depth along the fluvial to marine transition zone of tide-dominated river deltas: the need for a revision of depositional and hydraulic models. Earth-Sci. Rev. 191, 93–113.
Gugliotta, M., Saito, Y., Nguyen, V.L., Ta, T.K.O., Nakashima, R., Tamura, T., Uehara, K., Katsuki, K., Yamamoto, S., 2017. Process regime, salinity, morphological, and sedimentary trends along the fluvial to marine transition zone of the mixed-energy Mekong River delta, Vietnam. Cont. Shelf Res. 147, 7–26.
Gugliotta, M., Saito, Y., Nguyen, V.L., Ta, T.K.O., Tamura, T., Fukuda, S., 2018. Tide- and river-generated mud pebbles from the fluvial to marine transition zone of the Mekong River Delta, Vietnam. J. Sediment. Res. 88, 1–10.
Gugliotta, M., Saito, Y., Nguyen, V.L., Ta, T.K.O., Tamura, T., 2019. Sediment distribution and depositional processes along the fluvial to marine transition zone of the Mekong River delta, Vietnam. Sedimentology 66, 136–164.
Kanai, Y., Saito, Y., Tamura, T., Nguyen, V.L., Ta, T.K.O., Sato, A., 2013a. Sediment erosion revealed by study of Cs isotopes derived from the Fukushima Dai-ichi nuclear power plant accident. Geochem. J. 47, 79–82.
Kanai, Y., Saito, Y., Tamura, T., Nguyen, V.L., Ta, T.K.O., Sato, A., 2013b. Seasonal change of sedimentary environment in the Mekong Delta investigated by ^{7}Be, ^{210}Pb and radioactive Cs isotopes. Chikyukagaku (Geochemistry) 47, 89–100 (in Japanese, with English abstract).
Karlin, R., Levi, S., 1983. Diagenesis of magnetic minerals in recent haemipelagic sediments. Nature 303 (5915), 327–330.
Kohzu, A., Imai, A., Ohkouchi, N., Fukushima, T., Kamiya, K., Komatsu, K., Tomioka, N., Kawasaki, N., Miura, S., 2011. Direct evidence for the alteration of ^{13}C natural abundances during early diagenesis in Lake Kasumigaura, Japan. Geochem. Geophys. Geosyst. 12, Q10008. https://doi.org/10.1029/2011GC003532.
Kondolf, G.M., Rubin, Z.K., Minear, J.T., 2014. Dams on the Mekong: Cumulative sediment starvation. Water Resour. Res. 50, 5158–5169.
Kummu, M., Varis, O., 2007. Sediment-related impacts due to upstream reservoir trapping, the lower Mekong River. Geomorphology 85 (3), 275–293.
Lamb, A.L., Wilson, G.P., Leng, M.J., 2006. A review of coastal palaeoclimate and relative sea-level reconstructions using δ^{13}C and C/N ratios in organic material. Earth-Sci. Rev. 75 (1–4), 29–57.
McLachlan, R.L., Ogston, A.S., Allison, M.A., 2017. Implications of tidally-varying bed stress and intermittent estuarine stratification on fine-sediment dynamics through the Mekong's tidal river to estuarine reach. Cont. Shelf Res. 147, 27–37.
Mekong River Commission, 2005. Overview of the Hydrology of the Mekong Basin. Mekong River Commission, Vientiane, pp. 73.
Mekong River Commission, 2010. Technical Report on Land Cover Mapping 2010. http://portal.mrcmekong.org/tech_report.
Meyers, P.A., 1994. Preservation of elemental and isotopic source identification of sedimentary organic matter. Chem. Geol. 144 (3), 289–302.
Meyers, P.A., 1997. Organic geochemical proxies of paleoceanographic, paleolimnologic, and paleoclimatic processes. Org. Geochem. 27 (5–6), 213–250.
Milliman, J.D., Meade, R.H., 1983. World-wide delivery of river sediment to the oceans. J. Geol. 91, 1–21.
Nguyen, A.D., Savenije, H.H.G., Pham, D.N., Tang, D.T., 2008. Using salt intrusion measurements to determine the freshwater discharge distribution over the branches of a multi-channel estuary: the Mekong Delta case. Estuarine Coastal and Shelf Science 77 (3), 433–445.
Nguyen, C.T., 2013. Processes and Factors Controlling and Affecting the Retreat of Mangrove Shorelines in South Vietnam. (PhD thesis, Kiel).
Wolanski, E., Nhan, N.H., Spagnol, S., 1998. Sediment Dynamics during Low Flow Conditions in the Mekong River Estuary, Vietnam. J. Coast. Res. 14, 472–482.
Nguyen, V.L., Ta, T.K.O., Tateishi, M., 2000. Late Holocene depositional environments and coastal evolution of the Mekong River Delta, Southern Vietnam. J. Asian Earth Sci. 18 (4), 427–439.
Nittrouer, C.A., Austin, J.A., Field, M.E., Kravitz, J.H., Syvitski, J.P.M., Wiberg, P.L. (Eds.), 2007. Continental Margin Sedimentation: From Sediment Transport to Sequence Stratigraphy (IAS Special Publication 37). John Wiley, Chichester (560 p).
Nittrouer, C.A., Mullarney, J.C., Allison, M.A., Ogston, A.S., 2017a. Sedimentary processes building a tropical delta yesterday, today, and tomorrow: the Mekong system. Oceanography 30, 10–21.
Nittrouer, C.A., DeMaster, D.J., Eidam, E.F., Nguyen, T.T., Liu, J.P., Ogston, A.S., Phung, P.V., 2017b. The Mekong continental shelf: the primary sink for deltaic sediment particles and their passengers. Oceanography 30, 60–70.
Nowacki, D.J., Ogston, A.S., Nittrouer, C.A., Fricke, A.T., Tri, V.P.D., 2015. Sediment dynamics in the lower Mekong River: transition from tidal river to estuary. Journal of Geophysical Research Oceans 120 (9), 6363–6383.
Ogston, A.S., Allison, M.A., Mullarney, J.C., Nittrouer, C.A., 2017a. Sediment- and hydrodynamics of the Mekong Delta: from tidal river to continental shelf. Cont. Shelf Res. 147, 1–6.
Ogston, A.S., Allison, M.A., McLachlan, R.L., Nowacki, D.J., Stephens, J.D., 2017b. How tidal processes impact the transfer of sediment from source to sink: Mekong River collaborative studies. Oceanography 30, 22–33.
Oldfield, F., Crowther, J., 2007. Establishing fire incidence in temperate soils using magnetic measurements. Paleogeography, Palaeoclimatology, Palaeoecology 249, 362–369.
Oldfield, F., Asioli, A., Accorsi, C.A., Mercuri, A.M., Juggins, S., Langone, L., Rolph, T., Trincardi, F.T., Wolff, G., Gibbs, Z., Vigliotti, L., Frignani, M., van der Post, K., Branch, N., 2003. A high resolution late Holocene palaeo environmental record from the Central Adriatic Sea. Quat. Sci. Rev. 22, 319–342.
Pan, D., Chen, T., Zhan, Q., Wang, Z., 2017. Mineral magnetic properties of Holocene sediments in the subaqueous Yangtze delta and the implications for human activity and early diagenesis. Quat. Int. 459, 133–143.
Robinson, S.G., Sahota, J.T., Oldfield, F., 2000. Early diagenesis in North Atlantic abyssal plain sediments characterized by rock-magnetic and geochemical indices. Mar. Geol. 163, 77–107.
Sandbach, S.D., Nicholas, A.P., Ashworth, P.J., Best, J.L., Keevil, C.E., Parsons, D.R., Prokocki, E.K., Simpson, C.J., 2018. Hydrodynamic Modeling of Tidal-Fluvial Flows in a Large River Estuary. 212. pp. 176–188.
Snowball, I.F., 1993. Geochemical control of magnetite dissolution in subarctic lake sediments and the implications for environmental magnetism. J. Quat. Sci. 8, 339–346.
Ta, T.K.O., Nguyen, V.L., Tateishi, M., Kobayashi, I., Tanabe, S., Saito, Y., 2002. Holocene delta evolution and sediment discharge of the Mekong River, southern Vietnam. Quat. Sci. Rev. 21, 1807–1819.
Ta, T.K.O., Nguyen, V.L., Tateishi, M., Kobayashi, I., Saito, Y., 2005. Holocene delta evolution and depositional models of the Mekong River delta, southern Vietnam. In: Giosan, L., Bhattacharya, J.P. (Eds.), River Deltas – Concepts, Models, and Examples. SEPM Special Publication 83pp. 453–466.
Tamura, T., Horaguchi, K., Saito, Y., Nguyen, V.L., Tateishi, M., Ta, T.K.O., Nanayam, F., Watanabe, K., 2010. Monsoon-influenced variations in morphology and sediment of a mesotidal beach on the Mekong River delta coast. Geomorphology 116 (1–2), 11–23.
Tamura, T., Saito, Y., Bateman, M.D., Nguyen, V.L., Ta, T.K.O., Matsumoto, D., 2012a. Luminescence dating of beach ridges for characterizing multi-decadal to centennial deltaic shoreline changes during Late Holocene, Mekong River delta. Mar. Geol. 326, 140–153.
Tamura, T., Saito, Y., Nguyen, V.L., Ta, T.K.O., Bateman, M.D., Matsumoto, D., Yamashita, S., 2012b. Origin and evolution of interdistributary delta plains; insights from Mekong River delta. Geology 40, 303–306.
Thanh, V.Q., Reyns, J., Wackerman, C., Eidam, E.F., Roelvink, D., 2017. Modelling suspended sediment dynamics on the subaqueous delta of the Mekong River. Cont. Shelf Res. 213–230.
Thompson, R., Oldfield, F., 1986. Environmental Magnetism. Allen & Unwin, London.
Tri, V.K., 2012. Hydrology and Hydraulic Infrastructure Systems in the Mekong Delta, Vietnam. In: Renaud, F.G., Kuenzer, C. (Eds.), The Mekong Delta System, Interdisciplinary Analyses of a River Delta. Springer, pp. 49–82.
Wang, Z., Chen, Z., Li, M., Chen, J., Zhao, Y., 2009. Variations in downstream grain-sizes to interpret sediment transport in the middle-lower Yangtze River, China: a pre-study of Three-Gorges Dam. Geomorphology 113, 217–229.
Wang, Z., Li, M., Zhang, R., Liu, Y., Saito, Y., Xie, J., Li, B., Zhao, B., 2011a. Impacts of human activity on the late Holocene development of the subaqueous Yangtze delta, China, as shown by magnetic properties and sediment accumulation rates. The Holocene 21, 393–408.
Wang, J.J., Lu, X.X., Kummu, M., 2011b. Sediment load estimates and variations in the lower Mekong River. River Research & Applications 27, 33–46.
Wolanski, E., Nguyen, N.H., Dao, L.T., Nguyen, H.N., Nguyen, N.T., 1996. Fine-sediment Dynamics in the Mekong River Estuary, Vietnam. Estuar. Coast. Shelf Sci. 43, 565–582.